

# Dependence-based fuzzy clustering of functional time series

Ángel López-Oriona<sup>ID\*</sup> and Ying Sun<sup>ID</sup>

Statistics Program

King Abdullah University of Science and Technology (KAUST)

Thuwal, Saudi Arabia

Han Lin Shang<sup>ID</sup>

Department of Actuarial Studies and Business Analytics

Macquarie University

Sydney, Australia

## Abstract

Time series clustering is an important data mining task with a wide variety of applications. While most methods focus on time series taking values on the real line, very few works consider functional time series. However, functional objects frequently arise in many fields, such as actuarial science, demography or finance. Functional time series are indexed collections of infinite-dimensional curves viewed as random elements taking values in a Hilbert space. In this paper, the problem of clustering functional time series is addressed. To this aim, a distance between functional time series is introduced and used to construct a clustering procedure. The metric relies on a measure of serial dependence which can be seen as a natural extension of the classical quantile autocorrelation function to the functional setting. Since the dynamics of the series may vary over time, we adopt a fuzzy approach, which enables the procedure to locate each series into several clusters with different membership degrees. The resulting algorithm can group series generated from similar stochastic processes, reaching accurate results with series coming from a broad variety of functional models and requiring minimum hyperparameter tuning. Several simulation experiments show that the method exhibits a high clustering accuracy besides being computationally efficient. Two interesting applications involving high-frequency financial time series and age-specific mortality improvement rates illustrate the potential of the proposed approach.

*Keywords: Functional time series; Dependence measures; Clustering; Fuzzy C-medoids; Stock returns; Mortality improvement rates*

---

\*Postal address: CEMSE Division, Statistics Program, King Abdullah University of Science and Technology (KAUST), Thuwal 23955-6900, Saudi Arabia. E-mail: angel.lopezoriona@kaust.edu.sa

# 1 Introduction

Time series clustering concerns the problem of splitting a set of unlabeled time series into homogeneous groups so that similar series are placed together in the same group, and dissimilar series are located in different groups. The clustering task is frequently driven by the desired notion of similarity, which can be established in many ways. Usually, the purpose is to identify groups associated with similar generating mechanisms, which allows the characterization of a few dynamic patterns without the need to analyze and model each single time series in the collection, which is rarely the objective when dealing with a large number of series. The complexity inherent to objects evolving over time (e.g., the difficulty associated with determining a suitable dissimilarity principle or the existence of changes in the dynamic behaviors over time), together with the vast range of applications where time series clustering plays an essential role, justify a growing interest in this challenging topic. Comprehensive overviews including recent advances, promising prospects, classical references, and specific application areas, are provided by [Liao \(2005\)](#), [Aghabozorgi et al. \(2015\)](#), and [Maharaj et al. \(2019\)](#), to name a few.

Most clustering methods focus on real-valued time series. Among them, there are techniques based on discriminating between different geometric profiles of the time series ([Izakian et al. 2015](#), [Łuczak 2016](#)), model-based approaches ([Corduas and Piccolo 2008](#), [D’Urso et al. 2013](#), [D’Urso et al. 2016](#)), feature-based procedures ([D’Urso and Maharaj 2009](#), [D’Urso and Maharaj 2012](#), [López-Oriona, Vilar and D’Urso 2022](#), [López-Oriona, D’Urso, Vilar and Lafuente-Rego 2022a](#)), or methods based on reducing the dimensionality of the original time series as a preliminary step ([Singhal and Seborg 2005](#), [Pealat et al. 2021](#)). The suitability of each class of algorithms usually depends on the nature of the time series and the final goal of the user, with no approach dominating the remaining ones in every possible context. Regarding the cluster assignment criterion, two paradigms are considered according to whether a hard (also called crisp) or soft (also called fuzzy) partition is constructed.

Traditional clustering leads to hard solutions, where each data object is assigned to exactly one cluster. Overlapping groups are not allowed by hard partitions, which may not be suitable for many empirical applications where the cluster boundaries are not clearly determined or there are a few elements that are equidistant from some clusters. Soft clustering techniques provide a more versatile approach by considering the concept of membership of an object in a given group. In a soft partition, every element has an associated vector of membership degrees indicating the amount of confidence in the assignment to each cluster. A well-known approach to perform soft clustering is via classical fuzzy clustering algorithms ([Miyamoto et al. 2008](#)). Adopting the

fuzzy approach is usually advantageous when analyzing time series datasets, since changes in the dynamic patterns over time are frequent in practice. This becomes a challenge when dealing with a large number of time series because the underlying fuzzy partition can have a very high level of complexity.

A considerably smaller number of works have dealt with clustering time series having a range different from the real-valued. Among them, we can highlight some clustering algorithms for count time series (Etienne and Latifa 2014, Cerqueti et al. 2022) or categorical time series (Frühwirth-Schnatter and Pamminger 2010, García-Magariños and Vilar 2015), which are frequently employed for analyzing biological sequences. Another interesting type of time series currently considered in several fields is the so-called functional time series (e.g., Hörmann and Kokoszka 2012, Gao et al. 2019, Guo et al. 2022), which are indexed collections of infinite-dimensional curves belonging to a space of functions, commonly the Hilbert space. Functional time series are frequently used for the statistical analysis of certain types of data, such as intraday stock returns (Kokoszka and Zhang 2012, Horváth et al. 2014) or age-specific mortality rates (Hyndman and Shang 2009, Martínez-Hernández and Genton 2021), among others. While there are many works on clustering independent and identically distributed (i.i.d.) functional data, clustering of functional time series has received much less attention.

In the literature on i.i.d. functional data, cluster analysis is often coupled with dimension reduction techniques to address the curse of dimensionality. Garcia-Escudero and Gordaliza (2005) and Tarpey and Kinatader (2003) approximated the original data using fewer bases and then applied conventional clustering methods on the fitted basis function coefficients. However, such an approach can be problematic because it assumes the same basis functions for all clusters and the fitted coefficients preserve the clustering structures exhibited in the original functional data. To bypass this problem, Chiou and Li (2007) introduced  $k$ -centers functional clustering, which iteratively predicts and updates the group membership based on the estimated cluster structure. Using finite mixture, Bouveyron et al. (2015) proposed a functional mixture model-based clustering method to identify the common patterns between and within different bike-sharing systems. Chamroukhi et al. (2024) extended the modeling with Mixtures-of-Experts to the functional data analysis. Going from univariate to multivariate functional data, Bouveyron and Jacques (2011) extended high-dimensional data clustering to the functional case. Jacques and Preda (2014) considered clustering multivariate functional data. Both works assumed a Gaussian distribution for the principal component scores. All the previous methods are implicitly hindered by assuming the same basis functions for all clusters. For a review on model-based clustering and

classification of functional data, see [Chamroukhi and Nguyen \(2019\)](#).

With respect to the literature on high-dimensional functional time series clustering, to the best of our knowledge, the only work on the topic was provided by [Tang et al. \(2022\)](#), who constructed a novel technique based on functional panel data modeling to address the task of grouping functional time series of mortality rates in different countries. The proposed clustering method searches for homogeneous age-specific mortality rates of multiple countries by accounting for both the modes of variations and the temporal dynamics among curves. The empirical experiments performed by [Tang et al. \(2022\)](#) showed that the clustering results of age-specific mortality rates can be explained by the combination of geographic region, ethnic groups, and socioeconomic status. Additionally, the approach can be used to produce more accurate forecasts than several benchmark methods when predicting age-specific mortality rates. It is worth highlighting that, although the clustering technique of [Tang et al. \(2022\)](#) is powerful when dealing with curves of mortality rates, this procedure is not designed to group multiple functional time series in terms of their underlying temporal dependence structures.

Previous considerations highlight the need for clustering algorithms specifically constructed to deal with functional time series. Clustering of functional time series involves several challenges: (i) the inability of standard statistical methods to analyze functional data ([Ramsay and Silverman 2005](#), [Wang et al. 2016](#)), (ii) the difficulty inherent to the definition of dependence measures in a functional context ([Hörmann and Kokoszka 2010](#), [Valencia et al. 2019](#), [Kim and Kokoszka 2022](#)), and (iii) the high dimensionality of functional time series. These reasons explain a lack of works on the topic. In addition, given the complex nature of time series databases, it is beneficial to develop the fuzzy approach, whose versatility allows to capture changes in the dynamic behaviors of the series over time in real applications.

The main objective of this work is to introduce a fuzzy clustering algorithm for functional time series being able to: (i) group together functional time series coming from similar underlying processes, (ii) reach accurate results with series generated from a wide variety of functional processes, and (iii) efficiently perform the clustering task from a computational perspective.

To this aim, we first introduce a distance between functional time series. Since our goal is to group the time series according to their underlying structures, the dissimilarity relies on extracted features providing information about the serial dependence patterns. The computed features are based on a measure of serial dependence which can be seen as a natural extension of the classical quantile autocorrelation to the functional setting. Thus, the considered measure inherits the nice properties of the latter quantity in a clustering context, as the ability to identify complex

dependence patterns that standard correlation-based methods are unable to detect or the low computational complexity (Lafuente-Rego and Vilar 2016, Vilar et al. 2018, Lafuente-Rego et al. 2020). The introduced dissimilarity is used as input to the standard fuzzy C-medoids algorithm, which allows for the assignment of gradual memberships of the functional time series to clusters. Assessment of the clustering approach is carried out through some simulation experiments which consider data generated from different classes of functional processes. The performance of some alternative methods is also examined for comparison purposes.

The usefulness of the proposed approach is illustrated by means of two applications involving time series of intraday stock returns and age-specific mortality improvement rates. Particularly, the first case study considers functional time series of daily curves of 5-minute returns during the years 2018, 2019 and 2020, for several American companies belonging to two different sectors. We show that the procedure can differentiate between both sectors to some extent, with some time series displaying a considerable fuzzy behavior. The second case study involves functional time series of yearly curves of age-specific mortality improvement rates for different countries. Analyses are performed separately for the male, female, and total populations. The resulting clustering partitions lead to interesting interpretations related to certain characteristics of the considered countries. These applications indicate that: (i) the proposed measure of serial dependence can provide a significant understanding of the nature of the time series under study, and (ii) the clustering algorithm can produce a meaningful partition whose membership degrees give insights to practitioners about certain time series in the dataset.

The rest of the paper is organized as follows. A measure of serial dependence for functional processes and a distance between functional time series based on a proper estimate of this measure are introduced in Section 2. In Section 3, a fuzzy clustering algorithm based on the proposed metric is presented. The finite-sample performance of our proposed technique is analyzed in Section 4 through some simulation experiments where several alternative procedures are also assessed. Section 5 presents the applications of the proposed approach to the datasets of intraday stock returns and age-specific mortality improvement rates. Some concluding remarks are summarized in Section 6, along with some ideas on how the methodology can be further extended.

## 2 Measuring dissimilarity between functional time series

Let  $\{\mathcal{X}_t, t \in \mathbb{Z}\}$  be a strictly stationary stochastic process formed by real functional random variables taking values in the Hilbert space  $H = L^2(\mathcal{I})$ , with  $\mathcal{I} = [0, 1]$ , equipped with the inner

product  $\langle f, g \rangle = \int_0^1 f(u)g(u)du$ , for two functions  $f, g \in H$ . A distance between functional time series is defined after introducing a natural measure of serial dependence.

## 2.1 Measuring serial dependence in functional time series

Let us denote  $F_{\mathcal{X}(u)}$  as the marginal distribution function of the strictly stationary process  $\{\mathcal{X}_t(u), t \in \mathbb{Z}, u \in \mathcal{I} \subset \mathbb{R}\}$ , and  $q_\tau$  as the corresponding functional quantile of level  $\tau \in [0, 1]$ , that is,

$$q_\tau(u) = \inf\{x \in \mathbb{R} : F_{\mathcal{X}(u)}(x) \leq \tau\} \quad \text{for } u \in \mathcal{I}. \quad (1)$$

For a fixed lag,  $l \in \mathbb{Z}$ , a pair of quantile levels,  $(\tau, \tau') \in [0, 1]^2$ , and a pair of thresholds,  $(\beta, \beta') \in [0, 1]^2$ , consider the covariance between the indicator functions  $\mathbb{1}_\beta(\mathcal{X}_t, q_\tau)$  and  $\mathbb{1}_{\beta'}(\mathcal{X}_{t+l}, q_{\tau'})$  given by

$$\gamma(\tau, \tau', l, \beta, \beta') = \text{Cov} \left[ \mathbb{1}_\beta(\mathcal{X}_t, q_\tau), \mathbb{1}_{\beta'}(\mathcal{X}_{t+l}, q_{\tau'}) \right],$$

where

$$\mathbb{1}_\kappa(f, g) = \begin{cases} 1 & \text{if } \mathcal{L}(A) \leq \kappa, \\ 0 & \text{if } \mathcal{L}(A) > \kappa, \end{cases}$$

for two functions  $f, g \in H$  and  $\kappa \in [0, 1]$ , being

$$A = \{u \in \mathcal{I} : f(u) \leq g(u)\},$$

and  $\mathcal{L}$  the Lebesgue measure.

As the quantity  $\gamma(\tau, \tau', l, \beta, \beta')$  can be seen as an extension of the classical quantile autocovariance to the functional case, we term this quantity the *functional quantile autocovariance of lag  $l$  and thresholds  $\beta$  and  $\beta'$  for levels  $\tau$  and  $\tau'$* . Note that  $\gamma(\tau, \tau', l, \beta, \beta')$  can be expressed as

$$\gamma(\tau, \tau', l, \beta, \beta') = P(\mathcal{L}(A_\tau^t) \leq \beta, \mathcal{L}(A_{\tau'}^{t+l}) \leq \beta') - P(\mathcal{L}(A_\tau^t) \leq \beta)P(\mathcal{L}(A_{\tau'}^{t+l}) \leq \beta'),$$

where  $A_\alpha^t = \{u \in \mathcal{I} : \mathcal{X}_t(u) \leq q_\alpha(u)\}$  for  $\alpha \in [0, 1]$ , and that this quantity can be normalized to the interval  $[-1, 1]$  by considering

$$\rho(\tau, \tau', l, \beta, \beta') = \frac{\gamma(\tau, \tau', l, \beta, \beta')}{\left[ P(\mathcal{L}(A_\tau^t) \leq \beta)P(\mathcal{L}(A_{\tau'}^{t+l}) \leq \beta') [1 - P(\mathcal{L}(A_\tau^t) \leq \beta)] [1 - P(\mathcal{L}(A_{\tau'}^{t+l}) \leq \beta')] \right]^{1/2}},$$

which we refer to as the *functional quantile autocorrelation (FQA) of lag  $l$  and thresholds  $\beta$  and  $\beta'$  for levels  $\tau$  and  $\tau'$* . Note that  $\gamma(\tau, \tau', l, \beta, \beta')$  and  $\rho(\tau, \tau', l, \beta, \beta')$  take the value of zero for an i.i.d. functional process.

In practice, the previously defined quantities must be estimated from a  $T$ -length realization of the functional stochastic process  $\mathcal{X}_t$ ,  $\boldsymbol{\mathcal{X}}_T = (\mathcal{X}_1, \mathcal{X}_2, \dots, \mathcal{X}_T)$ , often referred to as *functional time series*. We will assume that each function in the realization is observed in a common set of  $p$  evenly spaced points,  $\mathfrak{U} = \{u_1, u_2, \dots, u_p\} \subset [0, 1]$ , with  $u_1 = 0$  and  $u_p = 1$ . Therefore, the information in the realization  $\boldsymbol{\mathcal{X}}_T$  can be expressed through the matrix

$$L = \begin{pmatrix} \mathcal{X}_1(u_1) & \mathcal{X}_1(u_2) & \cdots & \mathcal{X}_1(u_p) \\ \mathcal{X}_2(u_1) & \mathcal{X}_2(u_2) & \cdots & \mathcal{X}_2(u_p) \\ \vdots & \vdots & \ddots & \vdots \\ \mathcal{X}_T(u_1) & \mathcal{X}_T(u_2) & \cdots & \mathcal{X}_T(u_p) \end{pmatrix},$$

where  $\mathcal{X}_i(u_j)$  is the value of the function  $\mathcal{X}_i$  at the point  $u_j$ ,  $i = 1, \dots, T$ ,  $j = 1, \dots, p$ . Note that estimates of  $\gamma(\tau, \tau', l, \beta, \beta')$  and  $\rho(\tau, \tau', l, \beta, \beta')$  can be obtained by considering natural estimates of the probabilities  $P(\mathcal{L}(A_\tau^t) \leq \beta)$  and  $P(\mathcal{L}(A_\tau^t) \leq \beta, \mathcal{L}(A_{\tau'}^{t+l}) \leq \beta')$  given by

$$\begin{aligned} \widehat{P}(\mathcal{L}(A_\tau^t) \leq \beta) &= \frac{1}{T} \sum_{i=1}^T \mathbb{I}\left(\frac{\#\widehat{A}_\tau^i}{p} \leq \beta\right), \\ \widehat{P}(\mathcal{L}(A_\tau^t) \leq \beta, \mathcal{L}(A_{\tau'}^{t+l}) \leq \beta') &= \frac{1}{T-l} \sum_{i=1}^{T-l} \mathbb{I}\left(\frac{\#\widehat{A}_\tau^i}{p} \leq \beta\right) \mathbb{I}\left(\frac{\#\widehat{A}_{\tau'}^{i+l}}{p} \leq \beta'\right), \end{aligned}$$

respectively, where  $\mathbb{I}(\cdot)$  denotes the binary indicator function, the notation  $\#$  is used to indicate the cardinal of a set, and  $\widehat{A}_\alpha^k = \{u \in \mathfrak{U} : \mathcal{X}_k(u) \leq \widehat{q}_\alpha(u)\}$  for  $k = 1, \dots, T$  and  $\alpha \in [0, 1]$ , being  $\widehat{q}_\alpha(\cdot)$  the standard estimate of the  $\alpha^{\text{th}}$  quantile of a real functional random variable as defined in (1). The corresponding estimates for  $\gamma(\tau, \tau', l, \beta, \beta')$  and  $\rho(\tau, \tau', l, \beta, \beta')$  are denoted as  $\widehat{\gamma}(\tau, \tau', l, \beta, \beta')$  and  $\widehat{\rho}(\tau, \tau', l, \beta, \beta')$ , respectively.

A note on a natural choice for the thresholds  $\beta$  and  $\beta'$  in the previously introduced quantities is provided below.

*Remark 1. On the choice of the thresholds.* Note that the quantile levels  $\tau$  and  $\tau'$  provide a natural way of selecting the thresholds in the previously defined quantities by setting  $\beta = \tau$  and  $\beta' = \tau'$ . In such a case, since we have that  $P(\mathcal{L}(A_\alpha^t) \leq \alpha) = 0.5$  for any  $\alpha \in [0, 1]$ , the quantities can be expressed as

$$\begin{aligned} \gamma(\tau, \tau', l, \tau, \tau') &= P(\mathcal{L}(A_\tau^t) \leq \tau, \mathcal{L}(A_{\tau'}^{t+l}) \leq \tau') - 0.25, \\ \rho(\tau, \tau', l, \tau, \tau') &= \frac{\gamma(\tau, \tau', l, \tau, \tau')}{0.25}. \end{aligned}$$

Specifically,  $\gamma(\tau, \tau', l, \tau, \tau')$  can be seen as the simplest natural extension of the classical quantile autocovariance function (see, e.g., [Linton and Whang 2007](#), [Lee and Rao 2011](#), [Lafuente-Rego and Vilar 2016](#)) to the functional setting, since the latter quantity is also defined for a given lag and two different quantile levels.

## 2.2 A novel dissimilarity between functional time series

Suppose we have two strictly stationary functional processes  $\mathcal{X}_t^{(1)}$  and  $\mathcal{X}_t^{(2)}$ . A simple dissimilarity criterion to measure discrepancy between both processes consists in comparing their representations in terms of FQA evaluated for several lags on a common set of selected quantile levels and a common set of thresholds. Specifically, given a collection of  $L$  lags,  $\mathcal{L} = \{l_1, l_2, \dots, l_L\}$ , a collection of  $P$  quantile levels,  $\mathcal{T} = \{\tau_1, \tau_2, \dots, \tau_P\}$ , and a collection of  $B$  thresholds,  $\mathcal{B} = \{\beta_1, \beta_2, \dots, \beta_B\}$ , we define a distance  $d_{\text{FQA}} \in [0, 1]$  as

$$d_{\text{FQA}}(\mathcal{X}_t^{(1)}, \mathcal{X}_t^{(2)}) = \frac{1}{4LP^2B^2} \sum_{k=1}^L \sum_{i_1=1}^P \sum_{i_2=1}^P \sum_{j_1=1}^B \sum_{j_2=1}^B \left( \rho^{(1)}(\tau_{i_1}, \tau_{i_2}, l_k, \beta_{j_1}, \beta_{j_2}) - \rho^{(2)}(\tau_{i_1}, \tau_{i_2}, l_k, \beta_{j_1}, \beta_{j_2}) \right)^2,$$

where the superscripts  $(1)$  and  $(2)$  indicate that the corresponding quantities refer to the processes  $\mathcal{X}_t^{(1)}$  and  $\mathcal{X}_t^{(2)}$ , respectively.

In practice,  $d_{\text{FQA}}$  must be computed from realizations  $\boldsymbol{\mathcal{X}}_{T_1}^{(1)} = (\mathcal{X}_1^{(1)}, \mathcal{X}_2^{(1)}, \dots, \mathcal{X}_{T_1}^{(1)})$  and  $\boldsymbol{\mathcal{X}}_{T_2}^{(2)} = (\mathcal{X}_1^{(2)}, \mathcal{X}_2^{(2)}, \dots, \mathcal{X}_{T_2}^{(2)})$  of the stochastic processes  $\mathcal{X}_t^{(1)}$  and  $\mathcal{X}_t^{(2)}$ , respectively, by means of

$$\hat{d}_{\text{FQA}}(\mathcal{X}_t^{(1)}, \mathcal{X}_t^{(2)}) = \frac{1}{4LP^2B^2} \sum_{k=1}^L \sum_{i_1=1}^P \sum_{i_2=1}^P \sum_{j_1=1}^B \sum_{j_2=1}^B \left( \hat{\rho}^{(1)}(\tau_{i_1}, \tau_{i_2}, l_k, \beta_{j_1}, \beta_{j_2}) - \hat{\rho}^{(2)}(\tau_{i_1}, \tau_{i_2}, l_k, \beta_{j_1}, \beta_{j_2}) \right)^2.$$

A remark concerning the proposed dissimilarity is provided below.

*Remark 2. Advantages of feature-based distances.* The metric  $\hat{d}_{\text{FQA}}$  belongs to the class of feature-based distances, since it is based on comparing extracted features. The discriminative capability of this kind of distances mostly depend on selecting suitable features for a given context. Once a proper set of features is used, these distances present very nice properties such as dimensionality reduction, low computational complexity, robustness to the underlying models, and versatility to compare series with different lengths. Note that these properties are not satisfied by other dissimilarities between time series. For instance, metrics based on raw data usually involve high computational costs and require the series to have the same length, while model-based dissimilarities are expected to be extremely sensitive to model misspecification.

## 3 A fuzzy clustering algorithm for functional time series

We introduce a fuzzy clustering algorithm for functional time series based on the proposed distance  $\hat{d}_{\text{FQA}}$ .



### 3.1 A fuzzy C-medoids model based on the proposed dissimilarity

Let us consider a set of  $n$  functional time series,  $\mathcal{S} = \{\mathcal{X}_{T_1}^{(1)}, \dots, \mathcal{X}_{T_n}^{(n)}\}$ , where the  $i^{\text{th}}$  series has length  $T_i$ . We perform fuzzy clustering on the elements of  $\mathcal{S}$  in such a way that the series generated from similar stochastic processes are grouped together. To this aim, we propose to consider the fuzzy C-medoids clustering model introduced by Krishnapuram et al. (1999) in combination with the metric  $\widehat{d}_{\text{FQA}}$  proposed in Section 2.2. Thus, the goal is to determine the subset of  $\mathcal{S}$  of size  $C$ ,  $\widetilde{\mathcal{S}} = \{\widetilde{\mathcal{X}}^{(1)}, \dots, \widetilde{\mathcal{X}}^{(C)}\}$ , whose elements are usually referred to as medoids, and the  $n \times C$  matrix of fuzzy coefficients,  $\mathbf{U} = (u_{ic})$ , with  $i = 1, \dots, n$  and  $c = 1, \dots, C$ , leading to the solution of the minimization problem

$$\min_{\widetilde{\mathcal{S}}, \mathbf{U}} \sum_{i=1}^n \sum_{c=1}^C u_{ic}^m \times \widehat{d}_{\text{FQA}}(i, c), \quad \text{with respect to} \quad \sum_{c=1}^C u_{ic} = 1, u_{ic} \geq 0, \quad (2)$$

where  $\widehat{d}_{\text{FQA}}(i, c) = \widehat{d}_{\text{FQA}}(\mathcal{X}_{T_i}^{(i)}, \widetilde{\mathcal{X}}^{(c)})$ ,  $u_{ic} \in [0, 1]$  represents the membership degree of the  $i^{\text{th}}$  series in the  $c^{\text{th}}$  cluster, and  $m > 1$  is a real number, usually referred to as the fuzziness parameter, regulating the fuzziness of the partition. For  $m = 1$ , the crisp version of the algorithm is obtained, so the solution takes the form  $u_{ic} = 1$  if the  $i^{\text{th}}$  series pertains to cluster  $c$  and  $u_{ic} = 0$  otherwise. As the value of  $m$  increases, the boundaries between clusters get softer and the resulting partition is fuzzier.

The constrained optimization problem in (2) can be solved by means of the Lagrangian multipliers method, which leads to an iterative algorithm that alternately optimizes the membership degrees and the medoids. As stated in Höppner et al. (1999), the iterative solutions for the membership degrees are given by

$$u_{ic} = \left[ \sum_{c'=1}^C \left( \frac{\widehat{d}_{\text{FQA}}(i, c)}{\widehat{d}_{\text{FQA}}(i, c')} \right)^{\frac{1}{m-1}} \right]^{-1}. \quad (3)$$

Once the membership degrees are obtained through (3), the  $C$  series minimizing the objective function in (2) are selected as the new medoids. Specifically, for each  $c \in \{1, \dots, C\}$ , the index  $j_c$  satisfying

$$j_c = \arg \min_{1 \leq j \leq n} \sum_{i=1}^n u_{ic}^m \times \widehat{d}_{\text{FQA}}(\mathcal{X}_{T_i}^{(i)}, \mathcal{X}_{T_j}^{(j)}), \quad (4)$$

is computed. This two-step procedure is repeated until there is no change in the medoids or a maximum number of iterations is reached. An outline of the corresponding clustering algorithm is given in Algorithm 1. In the numerical analyses performed throughout the paper, the maximum number of iterations (parameter *max.iter* in Algorithm 1) was set to 100,000.

---

**Algorithm 1** Fuzzy C-medoids algorithm based on the distance  $\widehat{d}_{\text{FQA}}$ .

---

Fix  $C, m$  and  $\text{max.iter}$

Set  $\text{iter} = 0$

Pick the initial medoids,  $\widetilde{\mathcal{S}} = \{\widetilde{\mathcal{X}}^{(1)}, \dots, \widetilde{\mathcal{X}}^{(C)}\}$

**repeat**

Set  $\widetilde{\mathcal{S}}_{\text{OLD}} = \widetilde{\mathcal{S}}$

▷ Store the current medoids

Compute  $u_{ic}, i = 1, \dots, n, c = 1, \dots, C$ , using (3)

For each  $c \in \{1, \dots, C\}$ , determine the index  $j_c \in \{1, \dots, n\}$  using (4)

**return**  $\widetilde{\mathcal{X}}^{(c)} = \mathcal{X}_{T_{j_c}}^{(j_c)}$ , for  $c = 1, \dots, C$

▷ Update the medoids

$\text{iter} = \text{iter} + 1$

**until**  $\widetilde{\mathcal{S}}_{\text{OLD}} = \widetilde{\mathcal{S}}$  or  $\text{iter} = \text{max.iter}$


**return** The final fuzzy partition and the corresponding set of medoids

---

Two remarks related to the fuzzy C-medoids method described in Algorithm 1 are given below.

*Remark 3. Advantages of the fuzzy C-medoids model.* The fuzzy C-medoids procedure outlined in Algorithm 1 allows us to identify a set of representative functional time series belonging to the original collection, the medoids, whose overall distance to all other series in the set is minimal when the membership degrees with respect to a specific cluster are considered as weights (see the computation of  $j_c$  in Algorithm 1). As observed by Kaufman and Rousseeuw (2009), it is often desirable that the prototypes synthesising the structural information of each cluster belong to the original dataset, instead of obtaining virtual prototypes, as in the case of fuzzy C-means-based approaches (Dunn 1973, Bezdek 2013). For instance, the original set of series could be replaced by the set of medoids for exploratory purposes, thus substantially reducing the computational complexity of subsequent data mining tasks. The fuzzy C-medoids algorithm also exhibits classical advantages related to the fuzzy paradigm, including ability to produce richer clustering solutions than hard methods, to identify the vague nature of the prototypes, and to deal with time series sharing different dynamic patterns, among others.

*Remark 4. Hyperparameter selection in the fuzzy C-medoids model.* The fuzzy C-medoids procedure described in Algorithm 1 involves five hyperparameters: 1) the number of clusters,  $C$ , 2) the fuzziness parameter,  $m$ , 3) the collection of lags,  $\mathcal{L}$ , 4) the set of quantile levels,  $\mathcal{T}$ , and 5) the set of thresholds,  $\mathcal{B}$ . Concerning the set  $\mathcal{L}$ , we propose to select this set by using a mechanism analogous to the one described in López-Oriona, Vilar and D'Urso (2023, Section 3.4). Specifically, the procedure relies on assessing serial dependence at several lags for each functional time series.

To that aim, we employ an independence test based on the so-called distance correlation (Székely and Rizzo 2013), which is implemented via the function  $dcor.xy()$  of the  package `fda.usc` (Febrero-Bande and Oviedo de la Fuente 2012).

Regarding the set  $\mathcal{T}$ , we propose to consider  $\mathcal{T} = \{0.1, 0.5, 0.9\}$ , since this set is usually enough to achieve high accuracy when performing quantile-based time series clustering (Lafuente-Rego and Vilar 2016, Vilar et al. 2018, López-Oriona and Vilar 2021, López-Oriona, Vilar and D’Urso 2022). The set  $\mathcal{B}$  is selected as  $\mathcal{B} = \mathcal{T}$  (see Remark 1), since, during the numerical experiments performed in Section 4, this was the choice leading to the maximum value of the corresponding performance measures. Once the collections  $\mathcal{L}$ ,  $\mathcal{T}$  and  $\mathcal{B}$  have been selected, we propose to choose the parameters  $C$  and  $m$  by means of the following mechanism: (i) selecting a two-dimensional grid of values for the corresponding hyperparameters, (ii) running the clustering algorithm for each element in the grid and recording the associated fuzzy partition, and (iii) selecting the element leading to the minimum value of the Xie and Beni’s (1991) index. The lower this index, the better the fuzzy partition in terms of the compactness of the clusters and the separation between clusters. It is worth highlighting that this kind of criteria based on internal indexes have been used in several works on time series clustering to perform hyperparameter selection (López-Oriona, Vilar and D’Urso 2022, López-Oriona, Vilar and D’Urso 2023). Although a fixed choice for  $\mathcal{T}$  and  $\mathcal{B}$  was previously suggested, the above grid-search procedure could also be used to select these sets.

## 4 Simulation studies

We carry out a set of simulations with the aim of evaluating the behavior of the proposed approach in different scenarios of functional time series clustering. We describe some alternative methods that we consider for comparison purposes. We explain how the performance of the algorithms is measured, along with the corresponding simulation mechanisms and results. We also analyze the computational times associated with the proposed metric and the alternative approaches.

### 4.1 Alternative methods

To shed light on the behavior of the proposed clustering algorithm based on the distance  $\widehat{d}_{\text{FOA}}$  (see Section 3), we decided to compare this method with fuzzy  $C$ -medoids procedures relying on alternative dissimilarities. Specifically, we considered two metrics based on the (estimated) functional version of the Kendall correlation coefficient proposed by Valencia et al. (2019) adapted to the temporal setting. For a given functional time series,  $\mathcal{X}_T = (\mathcal{X}_1, \mathcal{X}_2, \dots, \mathcal{X}_T)$  and a lag  $l \in \mathbb{Z}$ ,

this quantity is defined as

$$\hat{\rho}_K(l) = \binom{T-l}{2}^{-1} \sum_{i=1}^{T-l} \sum_{j>i} [2\mathbb{I}(\mathcal{X}_i \prec \mathcal{X}_j)\mathbb{I}(\mathcal{X}_{i+l} \prec \mathcal{X}_{j+l}) + 2\mathbb{I}(\mathcal{X}_j \prec \mathcal{X}_i)\mathbb{I}(\mathcal{X}_{j+l} \prec \mathcal{X}_{i+l})] - 1,$$

where  $\prec$  denotes one of the following pre-orders for two continuous functions  $f$  and  $g$  defined in  $\mathcal{I}$ :


$$\begin{aligned} f \prec_m g &\equiv \max_{u \in \mathcal{I}} f(u) < \max_{u \in \mathcal{I}} g(u), \\ f \prec_i g &\equiv \int_0^1 (g(u) - f(u)) du > 0. \end{aligned} \tag{5}$$

Based on previous considerations, given the realizations  $\mathcal{X}_{T_1}^{(1)}$  and  $\mathcal{X}_{T_2}^{(2)}$  and the collection of lags  $\mathcal{L} = \{l_1, l_2, \dots, l_L\}$ , we define a (estimated) distance  $\hat{d}_K$  as

$$\hat{d}_K(\mathcal{X}_t^{(1)}, \mathcal{X}_t^{(2)}) = \frac{1}{4L} \sum_{k=1}^L \left( \hat{\rho}_K^{(1)}(l_k) - \hat{\rho}_K^{(2)}(l_k) \right)^2, \tag{6}$$

where the superscripts <sup>(1)</sup> and <sup>(2)</sup> indicate that the corresponding estimates are computed from the realizations  $\mathcal{X}_{T_1}^{(1)}$  and  $\mathcal{X}_{T_2}^{(2)}$ , respectively.

The pre-orders  $\prec_m$  and  $\prec_i$  defined in (5) give rise to two particular forms of the metric  $\hat{d}_K$ , which are denoted as  $\hat{d}_{K_m}$  and  $\hat{d}_{K_i}$ , respectively. The performance of the metrics  $\hat{d}_{K_m}$  and  $\hat{d}_{K_i}$  is an essential benchmark for the proposed distance, since they are both based on a measure of functional rank correlation, thus ignoring complex forms of functional dependence.

The proposed approach was also compared with the model-based clustering procedure introduced by Tang et al. (2022), which relies on a multilevel functional data model applied to functional panel data. Although this technique can not be directly associated with a distance measure, we will denote it as  $\hat{d}_{TSY}$ . It is worth highlighting that  $\hat{d}_{TSY}$  constitutes a hard clustering approach that automatically determines the number of clusters using a specific measure of within-cluster dispersion. In any case,  $\hat{d}_{TSY}$  can still be compared with the proposed approach in a reasonable manner in some of the simulation experiments (refer to Section 4.2.1). The approach  $\hat{d}_{TSY}$  is implemented via the function `mftsc()` of the  package `fts` (Hyndman and Shang 2024), which was employed for the analyses carried out throughout this section.

## 4.2 Experimental design and results

A comprehensive simulation study was carried out to evaluate the behavior of the fuzzy C-medoids algorithm based on the dissimilarity  $\hat{d}_{FQA}$ . We attempted to consider an evaluation process allowing to draw general conclusions about the performance of the distance. To this

aim, two different assessment schemes were designed. The first one includes scenarios with four different groups of functional time series, and is aimed at evaluating the ability of the procedure to assign a high (low) membership if a given functional time series pertains (not pertains) to a given group. The second one consists of scenarios constituted by two different groups of functional time series plus one additional series which does not belong to any of the groups. We examine again the membership degrees of the series in the two clusters, but also that the isolated series is not placed in any of the clusters with a high membership degree. In this context, a given threshold is used to determine whether or not a membership degree in a given cluster is enough to assign the functional time series to that group.

#### 4.2.1 First assessment scheme

We considered two scenarios consisting of four clusters represented by the same type of data generating processes, denoted by  $\mathcal{C}_1, \mathcal{C}_2, \mathcal{C}_3$  and  $\mathcal{C}_4$ . Each one of the groups contains five  $T$ -length functional time series, which gives rise to a set of 20  $T$ -length functional time series defining the true clustering partition. The data generating processes in each group are given below for each one of the scenarios.

**Scenario 1** Fuzzy clustering of functional time series generated from linear functional autoregressive (FAR) models (Bosq 2000). Let  $\{\mathcal{X}_t, t \in \mathbb{Z}\}$  be a functional stochastic process following the FAR(2) model given by

$$\mathcal{X}_t(u) = \int_0^1 \Gamma_1(u, v) \mathcal{X}_{t-1}(v) dv + \int_0^1 \Gamma_2(u, v) \mathcal{X}_{t-2}(v) dv + \epsilon_t(u),$$

where  $\Gamma_1(u, v) = c_1 \exp(-c_2(u^2 + v^2))$ ,  $\Gamma_2(u, v) = c_3 \exp(-c_4(u^2 + v^2))$ , with  $c_1, c_2, c_3, c_4 \in \mathbb{R}$ , and  $\epsilon_t(u)$  is an independent Brownian motion over  $[0, 1]$  with zero mean and variance  $1/T$ . The previous scenario is motivated by the first simulation setting in Wang and Cao (2023, Section 3). The vector of coefficients  $(c_1, c_2, c_3, c_4)$  is set as  $(-0.3, 0.1, 0, 0)$ ,  $(0.3, 0.3, 0, 0)$ ,  $(-0.4, 0.5, -0.3, 0.5)$ , and  $(0.4, 0.7, 0.3, 0.7)$  for clusters  $\mathcal{C}_1, \mathcal{C}_2, \mathcal{C}_3$  and  $\mathcal{C}_4$ , respectively.

**Scenario 2** Fuzzy clustering of functional time series generated from nonlinear models. Specifically, we considered a complex setting with two different types of processes: (i) nonlinear FAR processes, and (ii) functional GARCH (fGARCH) models proposed by Aue et al. (2017). The specific form of the considered processes is described below for each one of the classes:

- Let  $\{\mathcal{X}_t, t \in \mathbb{Z}\}$  be a functional stochastic process following the nonlinear FAR(1) model

given by

$$\mathcal{X}_t(u) = 0.75 \times \int_0^1 \Gamma_1(u, v) \mathcal{X}_{t-1}(v) dv \times \exp \left( \int_0^1 \Gamma_1(u, v) \mathcal{X}_{t-1}(v) dv \right) + \epsilon_t(u),$$

where  $\Gamma_1(u, v)$  and  $\epsilon_t(u)$  are defined as previously indicated. This scenario is motivated by the third simulation setting in [Wang and Cao \(2023, Section 3\)](#).

- Let  $\{\mathcal{X}_t, t \in \mathbb{Z}\}$  be a functional stochastic process following the fGARCH(1, 1) model given by the equations

$$\mathcal{X}_t(u) = \sigma_t(u) \epsilon_t(u),$$

$$\sigma_t^2(u) = \delta(u) + \alpha \mathcal{X}_{t-1}^2(u) + \beta \sigma_{t-1}^2(u),$$

where  $\{\epsilon_t, t \in \mathbb{Z}\}$  is a process formed by i.i.d. random functions and  $\delta$  is a nonnegative function. The integral operators  $\alpha$  and  $\beta$  are defined as  $(\alpha f)(u) = \int_0^1 \alpha(u, v) f(v) dv$ ,  $(\beta f)(u) = \int_0^1 \beta(u, v) f(v) dv$ , with  $u, v \in [0, 1]$ ,  $f \in H = L^2(\mathcal{I})$ , being  $\alpha(u, v)$  and  $\beta(u, v)$  elements of the Hilbert space  $H^2 = L^2(\mathcal{I}^2)$ . We consider  $\delta(u) = 0.01$ ,  $\alpha(u, v) = cu(1-u)v(1-v)$ ,  $\beta(u, v) = \alpha(u, v)$ , where  $c$  is a constant, and

$$\epsilon_t(u) = \frac{\sqrt{\ln 2}}{2^{200u}} B_t \left( \frac{2^{400u}}{\ln 2} \right),$$

with the process  $\{B_t, t \in \mathbb{Z}\}$  being formed by i.i.d. standard Brownian motions. The previous setting is motivated by the simulations experiments performed in [Aue et al. \(2017, Section 4\)](#) and [Huang and Shang \(2023, Section 3\)](#).

In Scenario 2, clusters  $\mathcal{C}_1$  and  $\mathcal{C}_2$  are associated with nonlinear FAR(1) models with vectors of coefficients  $(c_1, c_2) = (0.5, 0.5)$  and  $(c_1, c_2) = (0.9, 0.5)$ , respectively, while clusters  $\mathcal{C}_3$  and  $\mathcal{C}_4$  are associated with fGARCH(1, 1) models with  $c = 14$  and  $c = 15$ , respectively.

As an exploratory step, a metric two-dimensional scaling based on the metric  $\hat{d}_{\text{FQA}}$  was carried out to gain insight into the capability of this distance to discriminate between the underlying groups. Given a distance matrix  $\mathbf{D} = (D_{ij})_{1 \leq i, j \leq n}$ , a two-dimensional scaling finds the set of points  $\{(a_i, b_i), i = 1, \dots, n\}$  minimizing the loss function called stress given by

$$\sqrt{\frac{\sum_{i \neq j=1}^n (\| (a_i, b_i) - (a_j, b_j) \| - D_{ij})^2}{\sum_{i \neq j=1}^n D_{ij}^2}}.$$

The goal is to represent the distances  $D_{ij}$  in terms of Euclidean distances into a two-dimensional space so that the original distances are preserved as well as possible. The lower the value of the

stress function, the more reliable the two-dimensional scaling configuration. This way, a two-dimensional scaling plot provides a valuable visual representation of how the elements are located with respect to each other according to the original distance.

To obtain informative plots, 50 functional time series of length  $T = 1000$  were simulated from each generating model. The two-dimensional scaling was carried out for each set of 200 functional time series by computing the pairwise dissimilarity matrix based on  $\hat{d}_{\text{FQA}}$ . We considered the set of lags  $\mathcal{L} = \{1, 2\}$  in Scenario 1 and  $\mathcal{L} = \{1\}$  in Scenario 2. The resulting plots are shown in Figure 1, where different colors were used for each generating process. It is worth highlighting that the  $R^2$  value associated with the scaling is above 0.80 in both cases, thus concluding that the graphs in Figure 1 provide an accurate picture of the underlying representations according to the metric  $\hat{d}_{\text{FQA}}$ .

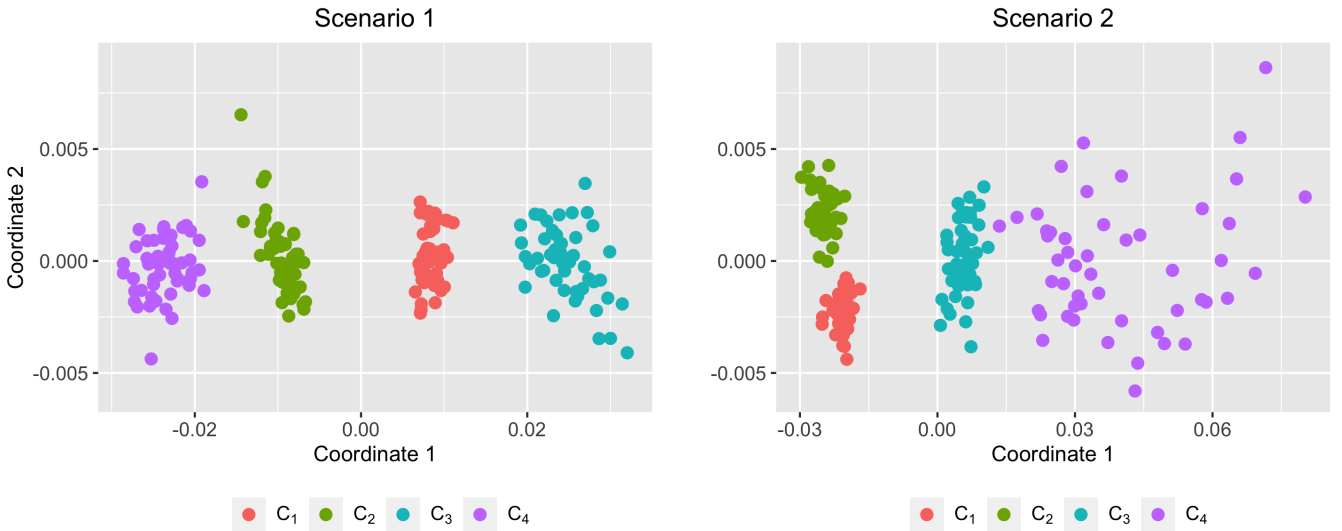


Figure 1: Two-dimensional scaling planes based on distance  $\hat{d}_{\text{FQA}}$  for Scenarios 1 and 2 considering series of length  $T = 1000$ .

The reduced bivariate spaces in Figure 1 show different configurations. In Scenario 1, the metric can differentiate between the four groups, which was expected due to the different model coefficients in the corresponding FAR processes. On the contrary, the two-dimensional scaling plot for Scenario 2 presents a configuration with a cluster ( $C_4$ ) whose elements are substantially spread out and three more compact groups, thus suggesting a challenging clustering setting.

The simulation study was carried out as follows. For each scenario, five functional time series of length  $T \in \{200, 600\}$  were generated from each process in order to execute the clustering algorithms twice and examine the effect of the series length. A number of  $p = 100$  discretization points evenly spaced on  $[0, 1]$  was used in all cases. Several values of the fuzziness parameter



$m$  were considered, namely  $m \in \{1.2, 1.4, 1.6, 1.8, 2\}$ . The problem of selecting a proper value for  $m$  has been extensively studied in the literature. However, there seems to be no consensus about the optimal way of choosing this parameter (see the discussion in [Maharaj and D'Urso 2011](#), Section 3.1.6). When  $m = 1$ , the hard version of the fuzzy C-medoids algorithm is obtained, while excessively large values of  $m$  result in a partition with all memberships close to  $1/C$  (highly overlapping groups). Consequently, selecting such values for  $m$  is not recommended ([Arabie et al. 1981](#)). Moreover, in the context of time series clustering, several works consider a grid of values for  $m$  similar to our choice ([D'Urso and Maharaj 2009](#), [Vilar et al. 2018](#), [López-Oriona and Vilar 2021](#), [López-Oriona, Weiß and Vilar 2023](#)).

Given a scenario and fixed values for  $m$  and  $T$ , 200 simulations were executed. In each trial, the fuzzy C-medoids algorithm based on  $\hat{d}_{\text{FQA}}$ ,  $\hat{d}_{\text{K}_m}$  and  $\hat{d}_{\text{K}_i}$  was applied using each value of  $m$  as input. The number of clusters was set to  $C = 4$ . The three dissimilarities were computed by employing the collection of lags  $\mathcal{L} = \{1, 2\}$  in Scenario 1 and  $\mathcal{L} = \{1\}$  in Scenario 2, thus considering the maximum number of defining lags at each scenario. For the computation of distance  $\hat{d}_{\text{FQA}}$ , the collections  $\mathcal{T}$  and  $\mathcal{B}$  were set as  $\{0.1, 0.5, 0.9\}$  (see [Remarks 1 and 4](#)). Moreover, the numerical experiments described throughout this section were also carried out by considering different choices for these sets, but no significant improvements were found.

In order to avoid the well-known issue of reaching local minima, the simulations were performed by considering the following two-step procedure:

- 1) Running the corresponding fuzzy C-medoids algorithm by using 200 different random starts for the set of initial medoids and storing the resulting membership matrix and medoids for each random start.
- 2) Among the 200 different clustering solutions, choosing the one giving rise to the minimum value of the objective function, refer to [\(2\)](#).

The idea of using several random initializations for the medoids and choosing the one leading to the optimal value of a given quantity (e.g., the objective function or a specific internal clustering quality index) has already been employed in some works on fuzzy clustering of time series ([López-Oriona, D'Urso, Vilar and Lafuente-Rego 2022b](#), [López-Oriona, Weiß and Vilar 2023](#)). In fact, this approach avoids the problem of having to choose a specific procedure for properly initializing the medoids.

Clustering accuracy was assessed using the fuzzy extensions of the Adjusted Rand Index (ARIF) and the Jaccard Index (JIF) introduced by [Campello \(2007\)](#). Both indexes are obtained



by reformulating the original ones in terms of the fuzzy set theory, which allows us to compare the true (hard) partition with an experimental fuzzy partition. ARIF and JIF take values on the intervals  $[-1, 1]$  and  $[0, 1]$ , respectively, with values closer to 1 indicating a more accurate clustering solution.

The method  $\hat{d}_{\text{TSY}}$  can not be directly compared with  $\hat{d}_{\text{FQA}}$ ,  $\hat{d}_{\text{K}_m}$  and  $\hat{d}_{\text{K}_i}$ . On the one hand, since  $\hat{d}_{\text{TSY}}$  constitutes a hard clustering approach and the current scenarios consider underlying hard partitions, this method is expected to naturally lead to higher values of ARIF and JIF than the alternative techniques. On the other hand,  $\hat{d}_{\text{TSY}}$  automatically determines the number of clusters in its first stage, which is a disadvantage with respect to  $\hat{d}_{\text{FQA}}$ ,  $\hat{d}_{\text{K}_m}$  and  $\hat{d}_{\text{K}_i}$ , since the latter methods use the true value  $C = 4$  as input. Hence, in order to carry out fair comparisons, we considered only the trials in which  $\hat{d}_{\text{TSY}}$  selected the true number of clusters ( $C = 4$ ).

The average values of ARIF and JIF based on the corresponding simulation trials are shown in the upper and lower parts of Table 1 for Scenarios 1 and 2, respectively. In both cases, the methods decrease their performance when increasing the value of  $m$ . This is reasonable and expected, since larger values of  $m$  produce a smoother boundary between the four well-separated clusters, thus making the classification fuzzier and resulting in lower values of ARIF and JIF. The method  $\hat{d}_{\text{TSY}}$  achieves substantially lower scores than the remaining approaches in all cases, which suggests that this technique is not appropriate to perform clustering when the differences are given by the dependence structures of the functional time series. To perform rigorous comparisons between  $\hat{d}_{\text{FQA}}$ ,  $\hat{d}_{\text{K}_m}$  and  $\hat{d}_{\text{K}_i}$ , pairwise paired  $t$ -tests were carried out by taking into account the 200 simulation trials. In each setting, the alternative hypotheses stated that the mean ARIF (JIF) value of a given method is greater than the mean ARIF (JIF) value of its counterpart. Bonferroni corrections were applied to the set of  $p$ -values associated with each scenario, clustering quality index, and value of  $T$ . An asterisk was incorporated in Table 1 if the corresponding method resulted: (i) no significantly worse than any other method for a significance level of 0.01, and (ii) significantly more effective than the ones without an asterisk for a significance level of 0.01.

Table 1: Average values of ARIF and JIF for several methods in Scenarios 1 and 2. For each value of  $m$  and  $T$ , the best result is shown in bold. An asterisk indicates that the corresponding method is more effective than the ones without an asterisk for a significance level of 0.01.

Scenario	$T$	$m$	ARIF				JIF			
			$\hat{d}_{\text{FQA}}$	$\hat{d}_{\text{K}_m}$	$\hat{d}_{\text{K}_i}$	$\hat{d}_{\text{TSY}}$	$\hat{d}_{\text{FQA}}$	$\hat{d}_{\text{K}_m}$	$\hat{d}_{\text{K}_i}$	$\hat{d}_{\text{TSY}}$
1	200	1.2	0.90	0.90	<b>0.94*</b>	0.23	0.86	0.87	<b>0.91*</b>	0.30
		1.4	0.80	0.88	<b>0.91*</b>	∅	0.74	0.83	<b>0.88*</b>	∅
		1.6	0.70	0.84	<b>0.88*</b>	∅	0.63	0.79	<b>0.83*</b>	∅
		1.8	0.61	0.79	<b>0.83*</b>	∅	0.55	0.73	<b>0.78*</b>	∅
		2.0	0.52	0.74	<b>0.79*</b>	∅	0.48	0.68	<b>0.72*</b>	∅
	600	1.2	<b>0.99</b>	<b>0.99</b>	<b>0.99</b>	0.27	<b>0.99</b>	<b>0.99</b>	<b>0.99</b>	0.35
		1.4	0.98	<b>0.99</b>	<b>0.99</b>	∅	0.97	0.98	<b>0.99</b>	∅
		1.6	0.93	0.97*	<b>0.98*</b>	∅	0.90	0.96*	<b>0.97*</b>	∅
		1.8	0.86	0.94*	<b>0.95*</b>	∅	0.81	0.92*	<b>0.93*</b>	∅
		2.0	0.78	<b>0.91*</b>	<b>0.91*</b>	∅	0.72	0.87*	<b>0.88*</b>	∅
2	200	1.2	<b>0.86*</b>	0.56	0.59	0.36	<b>0.81*</b>	0.50	0.53	0.35
		1.4	<b>0.78*</b>	0.52	0.55	∅	<b>0.72*</b>	0.47	0.50	∅
		1.6	<b>0.69*</b>	0.48	0.53	∅	<b>0.62*</b>	0.44	0.47	∅
		1.8	<b>0.61*</b>	0.45	0.50	∅	<b>0.55*</b>	0.41	0.44	∅
		2.0	<b>0.53*</b>	0.41	0.46	∅	<b>0.48*</b>	0.39	0.41	∅
	600	1.2	<b>0.99*</b>	0.70	0.68	0.41	<b>0.99*</b>	0.63	0.61	0.44
		1.4	<b>0.96*</b>	0.66	0.65	∅	<b>0.94*</b>	0.59	0.58	∅
		1.6	<b>0.90*</b>	0.62	0.63	∅	<b>0.86*</b>	0.55	0.56	∅
		1.8	<b>0.83*</b>	0.57	0.60	∅	<b>0.77*</b>	0.52	0.54	∅
		2.0	<b>0.76*</b>	0.53	0.57	∅	<b>0.69*</b>	0.48	0.51	∅

According to Table 1, the metrics based on functional autocorrelations,  $\hat{d}_{\text{K}_m}$  and  $\hat{d}_{\text{K}_i}$ , achieve a higher clustering accuracy than the proposed dissimilarity in Scenario 1, especially for large values of  $m$ . This was expected, since all the processes considered in this scenario display linear dependence structures. However, note that  $\hat{d}_{\text{FQA}}$  is able to reach almost perfect results when  $T = 600$  for small values of  $m$ , which is coherent with the two-dimensional scaling plot on the left panel of Figure 1. In Scenario 2, dissimilarity  $\hat{d}_{\text{FQA}}$  exhibits substantially greater clustering effectiveness than the remaining ones for all values of  $T$  and  $m$ , which suggests that the FQA-based features are more appropriate to perform clustering than the autocorrelation-based ones when the underlying groups are characterized by complex forms of functional dependence, as the ones produced by the fGARCH models. Specifically, the proposed distance achieves again very high

scores when  $T = 600$  in this challenging scenario associated with the two-dimensional scaling plot on the right panel of Figure 1.

#### 4.2.2 Second assessment scheme

A second simulation experiment was conducted to analyze the effect of ambiguous series, whose presence introduces a certain degree of uncertainty and increases the fuzzy nature of the clustering task. Two new scenarios consisting of two well-separated clusters of five functional time series each and a single isolated series arising from a different process are defined as follows.

**Scenario 3** A set of 11 functional time series, where five series are generated from a FAR(2) process with vector of coefficients  $(c_1, c_2, c_3, c_4) = (-0.4, 0.5, -0.4, 0.5)$ , five additional series are generated from a FAR(2) process with vector of coefficients  $(c_1, c_2, c_3, c_4) = (0.4, 0.5, 0.4, 0.5)$ , and one isolated series is generated considering an independent Brownian motion over  $[0, 1]$ .

**Scenario 4** A set of 11 functional time series, where five series are generated as in cluster  $\mathcal{C}_2$  of Scenario 2, five additional series are generated as in cluster  $\mathcal{C}_3$  of Scenario 2, and one isolated series is generated considering an independent Brownian motion over  $[0, 1]$ .

The values for  $T$ , the number of simulation trials, the number of discretization points, and the number of random starts for the set of medoids, as well as the sets  $\mathcal{L}$ ,  $\mathcal{T}$  and  $\mathcal{B}$ , were fixed as in Scenarios 1 and 2. The number of clusters was set to  $C = 2$ . The assessment was performed differently. We computed the proportion of times that the five series from cluster  $\mathcal{C}_1$  grouped together in one group, the five series from cluster  $\mathcal{C}_2$  clustered together in another group, and the isolated series had a relatively high membership degree with respect to both groups. To this aim, a cutoff point must be determined to conclude when a series is assigned to a specific cluster. We decided to use the cutoff value of 0.7, i.e., the  $i^{\text{th}}$  functional time series was placed into the  $c^{\text{th}}$  cluster if  $u_{ic} > 0.7$ . On the contrary, a time series was considered to simultaneously belong to both clusters if its membership degrees were below 0.7. The use of a cutoff value to assess fuzzy clustering algorithms has already been considered in prior works (Maharaj and D'Urso 2011, D'Urso and Maharaj 2012, López-Oriona, Vilar and D'Urso 2022, López-Oriona, Weiß and Vilar 2023). Specifically, some arguments for this choice are given in Maharaj and D'Urso (2011). As the method  $\hat{d}_{\text{TSY}}$  is a hard clustering approach, it was not considered in this second evaluation scheme.

This evaluation criterion is very sensitive to the selection of  $m$ , since a single series with membership degrees failing to fulfill the required condition results in an incorrect classification. In

fact, the different methods could achieve their best behaviour for rather different values of  $m$ . For this reason, we decided to run the clustering algorithms for a grid of values of  $m$  on a sufficiently large interval. Figure 2 contains the corresponding curves of rates of correct classification as a function of  $m$ .

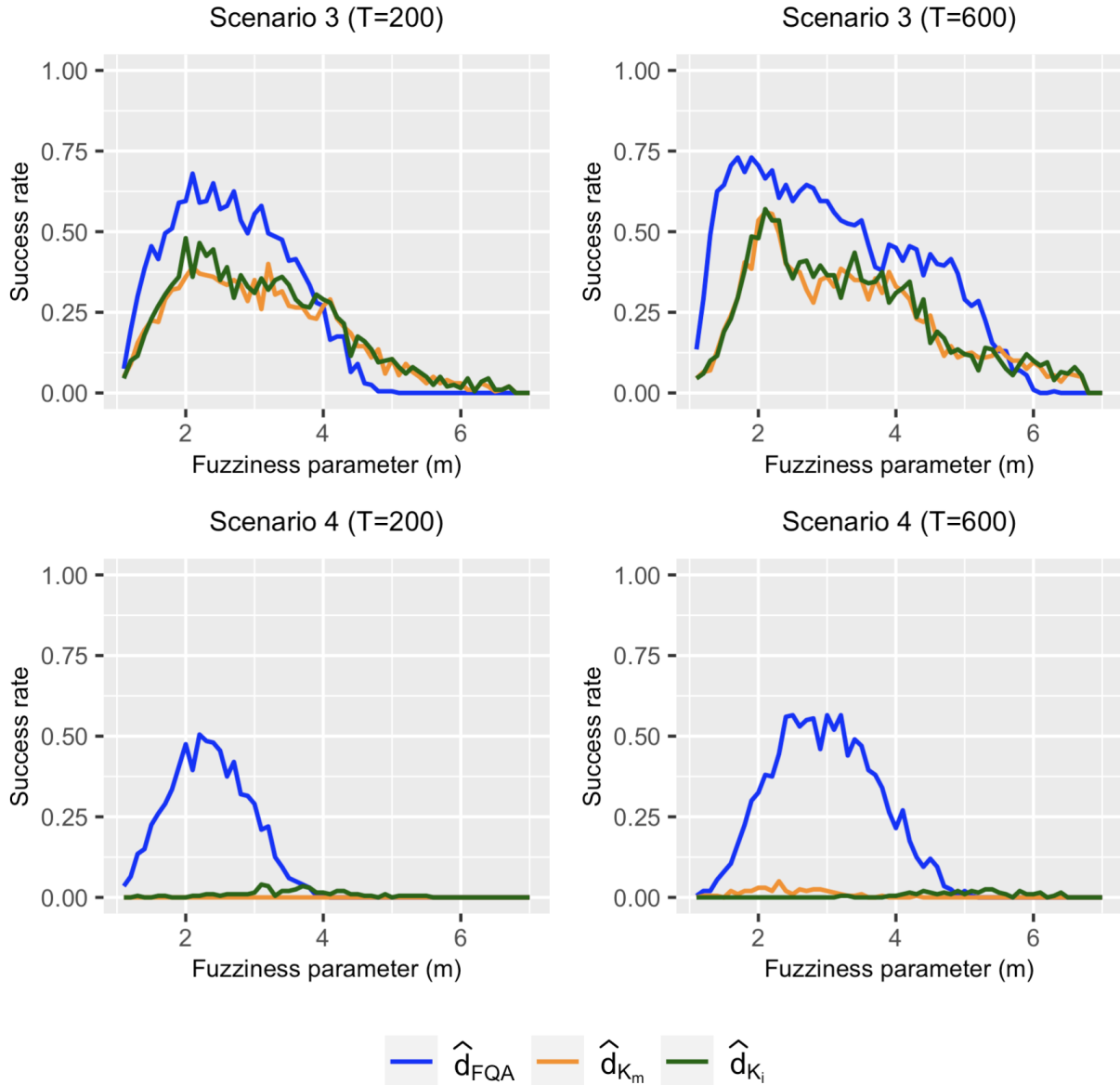


Figure 2: Rates of correct classification as a function of  $m$  obtained by the fuzzy  $C$ -medoids clustering algorithm based on three dissimilarities with a cutoff of 0.7. Scenarios 3 and 4.

The graphs in Figure 2 confirm that the fuzziness parameter dramatically affects the clustering performance. In all cases, low and high values of  $m$  produce poor rates of correct classification, since partitions with all memberships close to 1 or  $\frac{1}{2}$  are respectively returned, thus resulting in failed trials. On the contrary, moderate values of  $m$  generally result in higher clustering effectiveness, although the optimal range varies for each metric. In Scenario 3, the proposed

distance gets moderately better correct classification rates than the metrics based on functional autocorrelations, even though the models in this scenario are characterized by linear dependence structures. On the contrary, metric  $\hat{d}_{\text{FQA}}$  dramatically outperforms the alternative distances in Scenario 4. In particular,  $\hat{d}_{\text{K}_m}$  and  $\hat{d}_{\text{K}_i}$  attain close to 0 rates of correct classification even when long time series ( $T = 600$ ) are considered. In most cases, increasing the series length results in better rates of correct classification. Note that the previous results demonstrate the importance of a suitable selection of  $m$ , although this issue is not addressed here because there are several procedures available in the literature for this purpose.


Rigorous comparisons based on Figure 2 can be made by computing (i) the maximum value of each curve, and (ii) the area under each curve, denoted by the area under the fuzziness curve (AUFC), which was already used by López-Oriona, Vilar and D’Urso (2022) and López-Oriona, Weiß and Vilar (2023) in the context of fuzzy clustering of time series. The values for both quantities are given in Table 2, and corroborate the great performance of the proposed metric  $\hat{d}_{\text{FQA}}$  in Scenarios 3 and 4.

Table 2: Maximum rates of correct classification (MRCC) and AUFC obtained by the fuzzy C-medoids clustering algorithm based on three dissimilarities with a cutoff value of 0.7. Scenarios 3 and 4. The best results are shown in bold.

$T$	Metric	Scenario 3			Scenario 4		
		$\hat{d}_{\text{FQA}}$	$\hat{d}_{\text{K}_m}$	$\hat{d}_{\text{K}_i}$	$\hat{d}_{\text{FQA}}$	$\hat{d}_{\text{K}_m}$	$\hat{d}_{\text{K}_i}$
200	MRCC	<b>0.680</b>	0.400	0.480	<b>0.505</b>	0.000	0.040
	AUFC	<b>1.471</b>	1.069	1.153	<b>0.724</b>	0.000	0.046
600	MRCC	<b>0.730</b>	0.560	0.570	<b>0.565</b>	0.050	0.025
	AUFC	<b>2.216</b>	1.328	1.374	<b>1.133</b>	0.042	0.035

In summary, the experiments carried out throughout Section 4.2 indicate that the fuzzy C-medoids model based on  $\hat{d}_{\text{FQA}}$ : (i) shows competitive results with databases containing linear time series, being even able to outperform autocorrelation-based methods when the dataset includes ambiguous time series, and (ii) displays a substantially higher clustering accuracy than the alternative approaches when the underlying clusters are characterized by complex forms of functional dependence.

### 4.3 Computational time assessment

In order to analyze the efficiency of the four clustering approaches examined throughout Section 4, we recorded the runtime of the corresponding programs used for the experiments in Scenario 1. Specifically, given a method and a value for  $T$ , we reported the CPU runtime spent finishing the clustering task (for the five values of  $m$ ) regarding the 200 simulation trials. The computer used to run the programs was a MacBook Pro with an Apple M2 Pro chip and 16 GB of RAM. The programs were coded and executed in the  software (R Core Team 2024) (version 4.3.1).

The runtime (minutes) associated with each method is provided in Table 3. The fuzzy C-medoids method based on  $\hat{d}_{\text{FQA}}$  is associated with the lowest runtimes for both values of  $T$ . In contrast,  $\hat{d}_{\text{TSY}}$  is associated by far with the highest runtimes. Additionally, the computation time of the proposed approach barely increases with  $T$ . On the contrary, the runtime associated with distances  $\hat{d}_{\text{K}_m}$  and  $\hat{d}_{\text{K}_i}$  shows a substantial increase with  $T$ , which is expected, since the feature extraction mechanism of these metrics entails a number of  $\sum_{k=1}^L \binom{T-l_k}{2}$  comparisons. Among these two dissimilarities,  $\hat{d}_{\text{K}_i}$  is computationally heavier due to the integration involved in the definition of  $\prec_i$  in (5). In fact, the method based on  $\hat{d}_{\text{K}_i}$  could be infeasible to run in databases containing many time series of moderate to large lengths.

Table 3: Runtime (minutes) for the different methods regarding the 200 simulation trials in Scenario 1.

Method	$T = 200$	$T = 600$
$\hat{d}_{\text{FQA}}$	16.57	20.03
$\hat{d}_{\text{K}_m}$	26.17	212.81
$\hat{d}_{\text{K}_i}$	170.34	1545.17
$\hat{d}_{\text{TSY}}$	4590.14	32906.82

The above analyses show that the proposed clustering method is computationally efficient and can be feasibly executed even with databases containing long time series.

## 5 Financial and demographic applications

This section is devoted to showing two interesting applications of the proposed clustering procedure involving high-frequency financial time series and age-specific mortality improvement rates. In both cases, we first describe the considered data along with some exploratory analyses and, afterwards, we show the clustering results.

## 5.1 Clustering S&P 500 companies

We consider a dataset of closing prices of forty companies included in the S&P 500 index, which comprises some of the largest firms traded in the New York Stock Exchange. The stock prices are recorded in a 5-minute resolution (between 9:30 and 16:00 Eastern Standard Time for each trading day) and correspond to the period from 2 January 2018 to 31 December 2020. The data were sourced from the Refinitiv Datascope (<https://select.datascope.>). The considered companies belong to two different sectors, namely, the communication services (CS) sector and the energy (EN) sector. The name, symbol, and sector to which each company pertains are provided in Table 4.

This dataset was used to construct a collection of 40 functional time series (one for each company) by considering the daily curves of stock prices during the corresponding period. As the number of trading days in a given year is 252, and the prices are recorded in a 5-minute resolution during 6.5 hours each day, the corresponding functional time series have length  $T = 756$  and are observed on  $p = 78$  points. As the functional time series of prices are not stationary, these series are transformed into so-called intraday log-returns. Specifically, if  $P_{i,t}(u_j)$  is the intraday 5-minute closing price of the  $i^{\text{th}}$  company at time  $u_j$  on trading day  $t$ , the corresponding sequence of log-returns is defined as

$$R_{i,t}(u_j) = \ln P_{i,t}(u_j) - \ln P_{i,t}(u_{j-1}),$$

where  $i = 1, 2, \dots, 40$ ,  $j = 2, 3, \dots, 78$  and  $t = 1, 2, \dots, 756$ . In Figure 3, the first 100 curves (corresponding to 2018) of the functional time series of log-returns for the companies GOOGL and APA are displayed. Note that, although the values of the  $x$ -axis in these plots were chosen according to the daily trading times, the functional time series of log-returns are assumed to be defined in 77 evenly spaced points on the interval  $[0, 1]$ .

The stock returns are known to exhibit very complex forms of dependence beyond linearity (Hinich and Patterson 1985, Booth et al. 1994, Chen et al. 2005, Dahmene et al. 2021). Thus, since the proposed clustering algorithm showed the best performance with respect to the alternative methods when dealing with functional time series having complex dependence structures (see results for Scenarios 2 and 4 in Section 4.2), the considered functional time series of log-returns seem a very reasonable choice for the application of the procedure.

From a financial point of view, it is reasonable to believe that the temporal behavior of the log-return curves is influenced by the sector to which the corresponding company pertains. The analyses in López-Oriona and Vilar (2021, Section 5) suggest that the log-returns of the companies



Table 4: Summary of the 40 S&P 500 companies in the communication services (CS) sector (left) and the energy (EN) sector (right).

Company (CS sector)	Symbol	Company (EN sector)	Symbol
Alphabet Inc. A	GOOGL	APA Corporation	APA
Alphabet Inc. B	GOOG	Baker Hughes	BKR
AT&T	T	Chevron Corporation	CVX
Charter Communications	CHTR	Conoco Phillips	COP
Cisco Systems	CSCO	Devon Energy	DVN
Comcast	CMCSA	Diamondback Energy	FANG
Electronic Arts	EA	EOG Resources	EOG
Fox Corporation. A	FOXA	EQT Corporation	EQT
Fox Corporation. B	FOX	ExxonMobil	XOM
Interpublic Group of Companies	IPG	Halliburton	HAL
Live Nation Entertainment	LYV	Hess Corporation	HES
Meta Platforms	META	Kinder Morgan	KMI
Netflix	NFLX	Marathon Oil	MRO
News Corporation. A	NWSA	Marathon Petroleum	MPC
News Corporation. B	NWS	Occidental Petroleum	OXY
Omnicom Group	OMC	ONEOK	OKE
T-Mobile US	TMUS	Phillips 66	PSX
Take-Two Interactive	TTWO	Pioneer Natural Resources	PXD
Verizon	VZ	Schlumberger	SLB
Walt Disney	DIS	Valero Energy	VLO

belonging to some specific S&P 500 sectors exhibit a similar dynamic behavior. In addition, we expect to identify some series showing a vague behavior by considering a fuzzy approach.

The proposed clustering procedure was applied to the dataset of functional time series of log-returns considering  $C = 2$  to determine to what extent the algorithm can differentiate between the time series associated with both sectors. The remaining parameters (see Remark 4) were set as  $\mathcal{T} = \{0.1, 0.5, 0.9\}$ ,  $\mathcal{B} = \mathcal{T}$ ,  $\mathcal{L} = \{1\}$  and  $m = 1.8$ . Concerning  $\mathcal{L}$  and  $m$ , the considered values for the selection process were  $\mathcal{L} \in \{\{1\}, \{1, 2\}, \{1, 2, \dots, 10\}\}$  and  $m \in \{1.1, 1.2, \dots, 2\}$ .

As an exploratory exercise, we constructed a two-dimensional scaling plot based on the distance



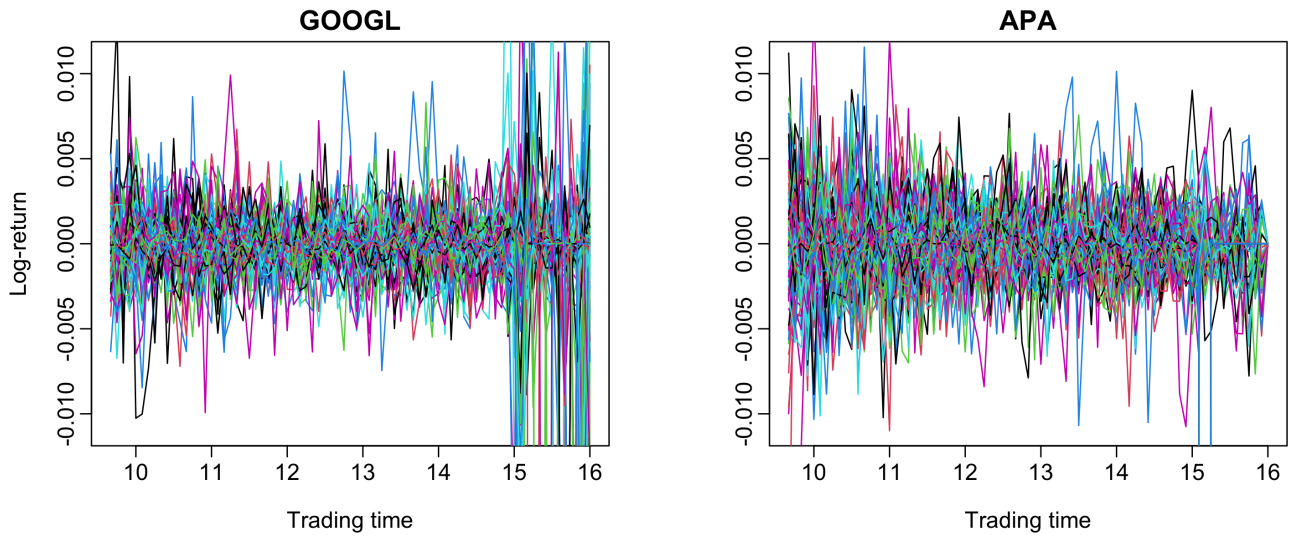


Figure 3: First 100 curves of the functional time series of log-returns for the companies GOOGL and APA.

$\hat{d}_{\text{FQA}}$ , whose computation was carried out using the above values for  $\mathcal{T}$ ,  $\mathcal{B}$  and  $\mathcal{L}$ . That way, a projection of the financial time series on a two-dimensional plane, preserving the original distances as well as possible, is available. The location of the 40 functional time series in the transformed space is displayed in Figure 4, where the points were colored according to the sector associated with each company.

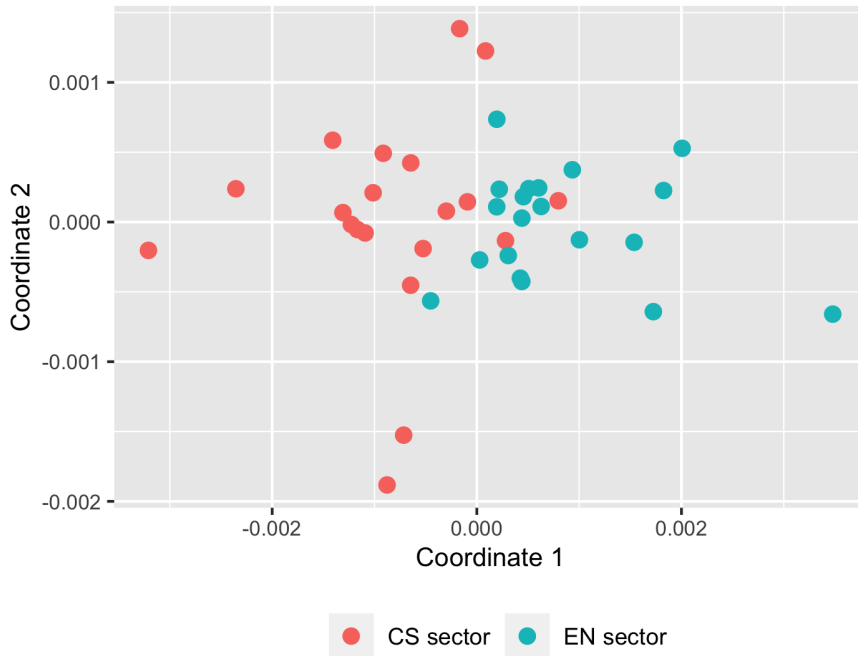


Figure 4: Two-dimensional scaling plane based on distance  $\hat{d}_{\text{FQA}}$  for the 40 functional time series of log-returns.

The two-dimensional scaling plot indicates that the distance  $\hat{d}_{\text{FQA}}$  can detect a certain structure

in the dataset related to the underlying sectors, since the points associated with CS and EN companies are concentrated in the left and right parts of the graph, respectively. However, there is a moderate degree of overlap between the two groups. In addition, in both cases, some series show a dynamic behavior that differs from the one characterizing their associated sectors. In sum, the configuration in Figure 4 suggests that the fuzzy approach could be appropriate for this dataset.

Table 5 contains the membership degrees produced by the fuzzy  $C$ -medoids clustering algorithm based on  $\hat{d}_{FQA}$ . Superscripts 1 and 2 in the name of the companies indicate the medoids according to clusters  $\mathcal{C}_1$  and  $\mathcal{C}_2$ , respectively. For the sake of interpretation, the maximum membership degree of each time series was highlighted in bold as long as it is greater than 0.7.

The clustering partition in Table 5 is consistent with the corresponding two-dimensional scaling plot in Figure 4. Cluster  $\mathcal{C}_1$  contains most of the companies of the CS sector, while the opposite occurs for cluster  $\mathcal{C}_2$  with the companies of the EN sector. In fact, more than half of the series in each group exhibit a maximum membership degree greater than 0.70, thus indicating that the underlying clustering structure is formed by moderately well-separated groups. However, there are 7 time series displaying a quite ambiguous behavior (i.e., with maximum membership degrees below 0.7), namely, the ones corresponding to the CS companies GOOGL, GOOG, T and TTWO, and to the EN companies BKR, EQT and HES. These functional time series share serial dependence structures characterizing both clusters, and the corresponding companies should be individually analyzed in order to understand the reason for the ambiguous behavior of their log-returns. Note that this type of insight can be reached due to the fuzzy nature of the partitions, remaining frequently hidden when considering crisp partitions. In addition, as expected from Figure 4, there are two CS companies showing a high membership degree in cluster  $\mathcal{C}_2$ , namely, LYV and OMC. The corresponding time series are associated with the two rightmost points in Figure 4. Such unexpected behavior could indicate the occurrence of uncommon phenomena in these companies during the corresponding years, although extracting such conclusions is beyond the scope of this paper.

For the sake of illustration and comparison purposes, we also obtained the clustering solutions according to the fuzzy  $C$ -medoids model based on the distances  $\hat{d}_{K_m}$  and  $\hat{d}_{K_i}$  considering  $C = 2$ . The selection of  $m$  was carried out similarly than in the above analyses, and the corresponding fuzzy partitions were obtained for the selected values for  $m$ , namely,  $m = 2$  for both  $\hat{d}_{K_m}$  and  $\hat{d}_{K_i}$ . Assuming that the true partition is given by the underlying sectors (CN and EN), the ARIF and JIF were obtained for both mentioned metrics as well as  $\hat{d}_{FQA}$ . Note that these quantities evaluate to what extent each dissimilarity is capable of separating the time series according to the

Table 5: Membership degrees of the 40 functional time series of log-returns produced by the fuzzy C-medoids model based on the metric  $\hat{d}_{\text{FQA}}$  for a two-cluster partition. The superscripts <sup>1</sup> and <sup>2</sup> indicate the medoid companies for clusters  $\mathcal{C}_1$  and  $\mathcal{C}_2$ , respectively. For each series, the maximum membership degree was highlighted in bold if it is greater than 0.7.

Company (CS sector)	$\mathcal{C}_1$	$\mathcal{C}_2$	Company (EN sector)	$\mathcal{C}_1$	$\mathcal{C}_2$
GOOGL	0.58	0.42	APA	0.09	<b>0.91</b>
GOOG	0.59	0.41	BKR	0.57	0.43
T	0.63	0.37	CVX	0.19	<b>0.81</b>
CHTR	<b>0.73</b>	0.27	COP	0.11	<b>0.89</b>
CSCO	<b>0.87</b>	0.13	DVN	0.12	<b>0.88</b>
CMCSA	<b>0.78</b>	0.22	FANG	0.18	<b>0.82</b>
EA	<b>0.71</b>	0.29	EOG	0.16	<b>0.84</b>
FOXA	<b>0.80</b>	0.20	EQT	0.31	0.69
FOX	<b>0.74</b>	0.26	XOM	0.17	<b>0.83</b>
IPG <sup>1</sup>	<b>1.00</b>	0.00	HAL	0.27	<b>0.73</b>
LYV	0.15	<b>0.85</b>	HES	0.43	0.57
META	<b>0.76</b>	0.24	KMI	0.15	<b>0.85</b>
NFLX	<b>0.76</b>	0.24	MRO <sup>2</sup>	0.00	<b>1.00</b>
NWSA	<b>0.90</b>	0.10	MPC	0.11	<b>0.89</b>
NWS	<b>0.86</b>	0.14	OXY	0.20	<b>0.80</b>
OMC	0.05	<b>0.95</b>	OKE	0.25	<b>0.75</b>
TMUS	<b>0.73</b>	0.27	PSX	0.18	<b>0.82</b>
TTWO	0.68	0.32	PXD	0.29	<b>0.71</b>
VZ	<b>0.74</b>	0.26	SLB	0.26	<b>0.74</b>
DIS	<b>0.82</b>	0.18	VLO	0.17	<b>0.83</b>

corresponding sectors in a crisp context. However, such values are clearly influenced by the choice of  $m$ , which is different among metrics. In order to circumvent this issue, we also computed the classical versions of the Adjusted Rand Index (ARI) and the Jaccard Index (JI) by transforming the corresponding fuzzy partitions into crisp partitions via the maximum membership rule.

The results are displayed in Table 6. The proposed metric achieves acceptable values for the fuzzy clustering indexes (ARIF and JIF), which was expected given the fuzzy partition in Table 5.

Table 6: Clustering quality indexes obtained by the fuzzy C-medoids procedures when grouping the 40 functional time series of log-returns. The ground truth is given by the corresponding sectors (CS and EN). The best results are shown in bold.

Metric	ARIF	JIF	ARI	JI
$\hat{d}_{\text{FQA}} (m = 1.8)$	0.33	0.49	<b>0.72</b>	<b>0.75</b>
$\hat{d}_{\text{Km}} (m = 2)$	0.24	0.46	0.23	0.47
$\hat{d}_{\text{Ki}} (m = 2)$	<b>0.37</b>	<b>0.53</b>	0.41	0.55

The autocorrelation-based metric  $\hat{d}_{\text{Ki}}$  attains slightly better scores for both indexes. However,  $\hat{d}_{\text{FQA}}$  reaches substantially higher values than  $\hat{d}_{\text{Ki}}$  in terms of the crisp clustering indexes (ARI and JI). These results corroborate that  $\hat{d}_{\text{FQA}}$  is indeed capable of detecting some structure in the functional time series dataset having an actual meaning in terms of industrial sectors.

When performing feature-based fuzzy clustering of time series, it is common to summarize the characteristics of the elements in each group by considering a weighted average of the considered features, with the weights given by the corresponding membership degrees. For a given cluster  $c \in \{1, 2\}$ , the dependence structures characterizing that group can be described through the set of features  $\{\bar{\rho}_c(\tau_1, \tau_2, 1, \tau_1, \tau_2) : \tau_1, \tau_2 \in \{0.1, 0.5, 0.9\}\}$ , with

$$\bar{\rho}_c(\tau_1, \tau_2, 1, \tau_1, \tau_2) = \frac{\sum_{i=1}^{40} u_{ic}^* \hat{\rho}^{(i)}(\tau_1, \tau_2, 1, \tau_1, \tau_2)}{\sum_{i=1}^{40} u_{ic}^*}, \quad (7)$$

where  $u_{ic}^*$  denotes the resulting membership degree of the  $i^{\text{th}}$  functional time series in the  $c^{\text{th}}$  cluster according to the fuzzy partition produced by  $\hat{d}_{\text{FQA}}$  (see Table 5).

Table 7: Values of  $\bar{\rho}_c(\tau_1, \tau_2, 1, \tau_1, \tau_2)$  for the two-cluster solution produced by  $\hat{d}_{\text{FQA}}$  with the 40 functional time series of log-returns.

$\mathcal{C}_1$	$\tau_2$			$\mathcal{C}_2$	$\tau_2$		
	0.1	0.5	0.9		0.1	0.5	0.9
$\tau_1 = 0.1$	0.51	-0.08	-0.54	$\tau_1 = 0.1$	0.60	-0.09	-0.62
$\tau_1 = 0.5$	-0.07	0.08	0.07	$\tau_1 = 0.5$	-0.08	0.13	0.09
$\tau_1 = 0.9$	-0.50	0.09	0.53	$\tau_1 = 0.9$	-0.58	0.10	0.59

The above-introduced quantities are given in Table 7. All the considered values are similar for both clusters, which indicates that the 40 functional time series of log-returns exhibit a quite

homogeneous dynamic behavior, thus highlighting the complexity of the clustering task. However, slight-to-moderate differences can be observed for some of the quantities. Specifically, the highest discrepancies occur when  $(\tau_1, \tau_2) \in \{(0.1, 0.1), (0.1, 0.9), (0.9, 0.1)\}$ . Note that all the features associated with  $\mathcal{C}_2$  are larger, in absolute value, than the ones associated with  $\mathcal{C}_1$ , which suggests that the functional time series in the second group (EN sector) display a stronger degree of serial dependence. In addition, although interpreting these quantities is not straightforward, a careful analysis of the corresponding values could give the practitioner a general picture of the different dynamics displayed by the companies in both sectors.

## 5.2 Clustering age-specific mortality improvement rates

We consider age-specific mortality rates in forty-one countries over several years. The mortality rates are the ratios of death counts to population exposure in the relevant year for a given age interval. Specifically, we examine age groupings ranging from 0 to 110 in single years of age, with the last age group including all ages of 110 and above. The data were sourced from the [Human Mortality Database \(2024\)](#). As the available sample period differs among the forty-one countries, and there are some countries with only a few years of available data, we decided to consider only the countries for which we have mortality data at least since 1960. For such countries, our sample period is from 1960 till the last year of available data, which varies among countries. Among the original ones, 33 countries were selected, namely Australia (AUS), Austria (AUT), Belarus (BLR), Belgium (BEL), Bulgaria (BGR), Canada (CAN), Czech Republic (CZE), Denmark (DNK), Estonia (EST), Finland (FIN), France (FRA), Hungary (HUN), Iceland (ISL), Ireland (IRL), Italy (ITA), Japan (JPN), Latvia (LVA), Lithuania (LTU), Luxembourg (LUX), Netherlands (NLD), New Zealand (NZL), Norway (NOR), Poland (POL), Portugal (PRT), Russia (RUS), Slovakia (SVK), Spain (ESP), Sweden (SWE), Switzerland (CHE), Taiwan (TWN), the United Kingdom (GBR), Ukraine (UKR) and the United States (USA).

The mortality data from the selected countries were used to construct a collection of 33 functional time series by considering the yearly curves of mortality rates as a function of age. As the 33 countries are associated with different ending years, our series have different lengths, which vary from  $T = 54$  (UKR) to  $T = 64$  (DNK). These series were smoothed by using the function `smooth.demogdata()` of the [R](#) package **demography** (Hyndman 2023), tailored to handle any missing value or poor data quality issues at the higher ages. As the smoothed functional time series of mortality rates are not stationary, the series were transformed into so-called mortality improvement rates (Haberman and Renshaw 2012, Shang 2019). Specifically, if  $M_{i,t}(u_j)$  is the

smoothed mortality rate of the  $i^{\text{th}}$  country for age  $u_j$  on year  $t$ , the series of mortality improvement rates is defined as

$$M_{i,t}^*(u_j) = 2 \times \frac{M_{i,t-1}(u_j) - M_{i,t}(u_j)}{M_{i,t-1}(u_j) + M_{i,t}(u_j)},$$

where  $i = 1, 2, \dots, 33$ ,  $j = 0, 1, \dots, 110$  and  $t = 2, 3, \dots, L_i$ , being  $L_i$  the length of the series of mortality rates for the  $i^{\text{th}}$  country. For demonstration, the functional time series of mortality improvement rates for JPN and RUS are displayed in Figure 5.

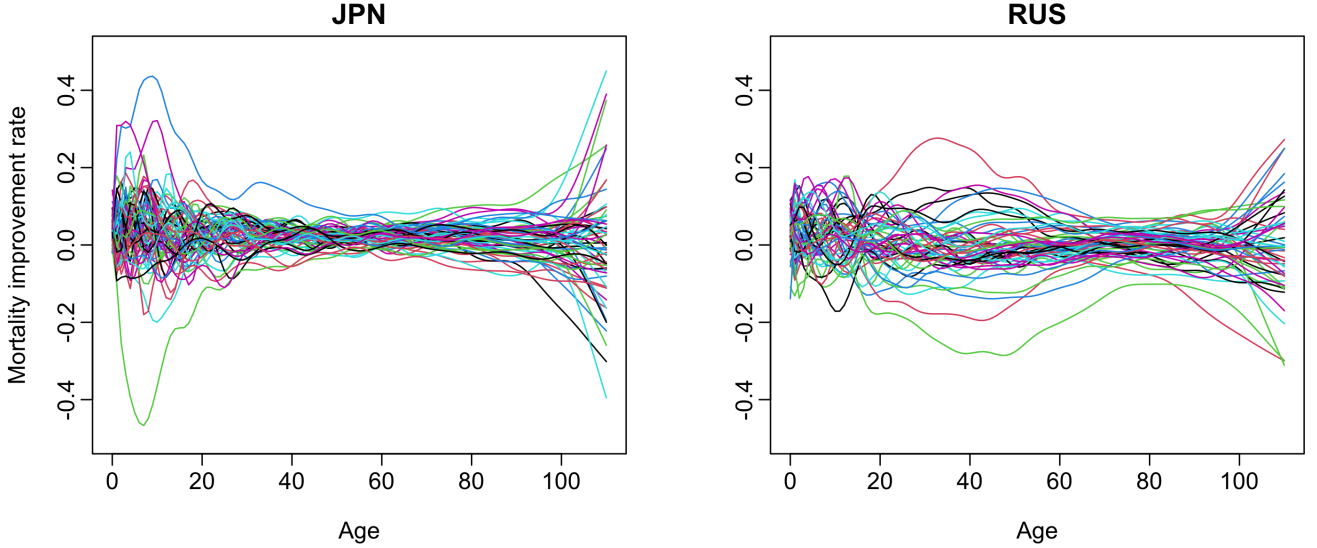


Figure 5: Functional time series of mortality improvement rates for JPN (from 1960 to 2022) and RUS (from 1960 to 2014).

We applied the proposed clustering procedure to the dataset of 33 functional time series of mortality improvement rates. As in the above application, and, according to Remark 4, the sets  $\mathcal{T}$  and  $\mathcal{B}$  were selected as  $\mathcal{T} = \{0.1, 0.5, 0.9\}$  and  $\mathcal{B} = \mathcal{T}$ . The collection of lags,  $\mathcal{L}$ , was set to  $\mathcal{L} = \{1\}$ . This time, as the number of clusters was not fixed in advance, the values of  $C$  and  $m$  were selected simultaneously through the criterion based on internal clustering quality indexes described in Remark 4, resulting  $C = 2$  and  $m = 1.5$ . The grids considered for the selection of  $\mathcal{L}$  and  $m$  were the same as in the previous application. The grid associated with the number of groups was given by the set  $\{2, \dots, 6\}$ .

The clustering partition produced by the proposed algorithm is given in the left part of Table 8, where the bold font has the same meaning as in the above application. As expected from the selected value for  $m$ , the highest membership degree is close to one for almost all countries, thus suggesting an underlying clustering configuration with a low degree of fuzziness. Cluster  $\mathcal{C}_1$  contains many European countries along with AUS, NZL and TWN. Cluster  $\mathcal{C}_2$  includes BLR, RUS and UKR, along with the North American countries CAN and USA, the Baltic states EST, LVA

and LTU, and SVK. It is worth highlighting that this second group makes a lot of sense from a geographical and political point of view. For instance, the six neighboring countries BLR, RUS, UKR, EST, LVA and LTU belonged until 1991 to the same state, the Soviet Union. Therefore, it is not surprising that the mortality improvement rates in these countries show a similar dynamic behavior during the last 60 years. The only country with membership degrees substantially spread out is JPN, whose mortality improvement rates share some patterns with the series in both groups.

Table 8: Membership degrees of the 33 functional time series of mortality improvement rates produced by the fuzzy  $C$ -medoids model based on the metric  $\hat{d}_{FQA}$ . The left, middle, and right parts show the partitions associated with the total, male and female populations, respectively. For each series, the maximum membership degree was highlighted in bold if it is greater than 0.7.

Country	Total		Male		Female					
	$C_1$	$C_2$	$C_1$	$C_2$	$C_1$	$C_2$	$C_3$	$C_4$	$C_5$	$C_6$
AUS	<b>0.88</b>	0.12	<b>0.98</b>	0.02	0.07	0.05	0.10	0.05	0.21	0.52
AUT	<b>0.88</b>	0.12	<b>0.94</b>	0.06	0.36	0.12	0.12	0.02	0.34	0.04
BLR	0.22	<b>0.78</b>	<b>0.97</b>	0.03	0.01	<b>0.91</b>	0.01	0.01	0.04	0.02
BEL	<b>0.92</b>	0.08	<b>0.94</b>	0.06	0.08	0.04	0.17	0.04	0.33	0.34
BGR	<b>0.93</b>	0.07	<b>0.98</b>	0.02	0.00	0.00	0.00	0.00	<b>1.00</b>	0.00
CAN	0.10	<b>0.90</b>	<b>0.86</b>	0.14	0.05	0.58	0.07	0.05	0.09	0.16
CZE	<b>0.86</b>	0.14	<b>1.00</b>	0.00	0.28	0.05	0.48	0.02	0.09	0.08
DNK	<b>0.95</b>	0.05	<b>0.97</b>	0.03	0.31	0.07	0.05	0.01	0.29	0.27
EST	0.25	<b>0.75</b>	<b>0.96</b>	0.04	0.09	0.46	0.30	0.02	0.07	0.06
FIN	<b>0.93</b>	0.07	<b>0.99</b>	0.01	0.11	0.03	0.18	0.04	0.18	0.46
FRA	<b>0.96</b>	0.04	<b>0.84</b>	0.16	0.08	0.08	0.09	0.23	0.46	0.06
HUN	<b>0.80</b>	0.20	<b>0.99</b>	0.01	0.00	0.00	0.00	0.00	0.00	<b>1.00</b>
ISL	0.68	0.32	0.00	<b>1.00</b>	0.12	0.14	0.14	0.11	0.24	0.25
IRL	<b>0.89</b>	0.11	<b>0.95</b>	0.05	0.04	0.05	0.22	0.04	0.12	0.53
ITA	<b>0.93</b>	0.07	<b>0.96</b>	0.04	0.37	0.05	0.20	0.02	0.29	0.07
JPN	0.53	0.47	<b>0.99</b>	0.01	0.00	<b>1.00</b>	0.00	0.00	0.00	0.00
LVA	0.06	<b>0.94</b>	<b>0.95</b>	0.05	0.33	0.14	0.43	0.06	0.03	0.01
LTU	0.18	<b>0.82</b>	<b>0.92</b>	0.08	0.14	0.33	0.30	0.17	0.03	0.03
LUX	<b>0.93</b>	0.07	<b>0.87</b>	0.13	0.22	0.17	0.17	0.04	0.30	0.10

Continued on next page



Country	Total		Male		Female					
	$\mathcal{C}_1$	$\mathcal{C}_2$	$\mathcal{C}_1$	$\mathcal{C}_2$	$\mathcal{C}_1$	$\mathcal{C}_2$	$\mathcal{C}_3$	$\mathcal{C}_4$	$\mathcal{C}_5$	$\mathcal{C}_6$
NLD	<b>0.92</b>	0.08	<b>0.99</b>	0.01	0.12	0.04	0.10	0.17	0.55	0.02
NZL	<b>0.93</b>	0.07	<b>1.00</b>	0.00	0.25	0.09	0.25	0.08	0.20	0.13
NOR	<b>0.78</b>	0.22	<b>0.97</b>	0.03	0.00	0.00	0.00	<b>1.00</b>	0.00	0.00
POL	<b>0.96</b>	0.04	<b>0.96</b>	0.04	0.02	0.20	0.03	0.11	0.26	0.38
PRT	<b>1.00</b>	0.00	<b>0.98</b>	0.02	0.21	0.19	0.14	0.21	0.15	0.10
RUS	0.12	<b>0.88</b>	<b>0.82</b>	0.18	0.08	0.49	0.11	0.08	0.16	0.08
SVK	0.25	<b>0.75</b>	<b>0.99</b>	0.01	0.00	0.00	<b>1.00</b>	0.00	0.00	0.00
ESP	<b>0.96</b>	0.04	<b>0.98</b>	0.02	0.06	0.25	0.20	0.26	0.21	0.02
SWE	<b>0.94</b>	0.06	<b>0.99</b>	0.01	<b>1.00</b>	0.00	0.00	0.00	0.00	0.00
CHE	<b>0.89</b>	0.11	<b>0.99</b>	0.01	0.29	0.07	0.42	0.12	0.04	0.06
TWN	<b>0.97</b>	0.03	<b>0.95</b>	0.05	0.46	0.09	0.04	0.09	0.29	0.03
GBR	<b>0.95</b>	0.05	<b>0.99</b>	0.01	0.05	0.03	0.07	0.08	0.52	0.25
UKR	0.01	<b>0.99</b>	<b>0.87</b>	0.13	0.02	<b>0.81</b>	0.06	0.07	0.03	0.01
USA	0.00	<b>1.00</b>	<b>0.96</b>	0.04	0.01	<b>0.83</b>	0.13	0.01	0.01	0.01

From (7), we decided to summarize the characteristics of the countries in each group via weighted averages of the corresponding FQA-based features. These quantities are given in the top part of Table 9.

Cluster  $\mathcal{C}_1$  is associated with higher absolute values in almost all cases, thus indicating that the mortality improvement rates of the countries in this cluster show a stronger degree of serial dependence. On the other hand, most values for cluster  $\mathcal{C}_2$  are close to zero. Therefore, the series in this cluster could be assumed to be generated from a stochastic process which is close to an i.i.d. process, thus indicating, for instance, that the yearly curves of mortality improvement rates for the corresponding countries are hard to predict from past information.

As an additional exploratory exercise, we decided to repeat the above analyses considering the 33 functional time series of mortality improvement rates for the male and female populations separately. The hyperparameter selection procedure described in Remark 4 resulted in  $\mathcal{L} = \{1\}$ ,  $C = 2$  and  $m = 1.5$  for the male data and in  $\mathcal{L} = \{1, 2\}$ ,  $C = 6$  and  $m = 1.3$  for the female data.

The clustering partitions associated with the male and female populations are given in the middle and right parts of Table 8, respectively. Note that, even though the clustering solution for



Table 9: Values of  $\bar{\rho}_c(\tau_1, \tau_2, 1, \tau_1, \tau_2)$  for two-cluster solutions produced by  $\hat{d}_{\text{FQA}}$  with the 33 functional time series of mortality improvement rates. The top and bottom parts are associated with the total and male populations, respectively.

Total				Total			
$\mathcal{C}_1$	$\tau_2$	$\tau_2$	$\tau_2$	$\mathcal{C}_2$	$\tau_2$	$\tau_2$	$\tau_2$
	0.1	0.5	0.9		0.1	0.5	0.9
$\tau_1 = 0.1$	-0.06	-0.14	-0.17	$\tau_1 = 0.1$	0.05	0.01	-0.04
$\tau_1 = 0.5$	-0.12	-0.18	-0.15	$\tau_1 = 0.5$	0.00	0.03	0.01
$\tau_1 = 0.9$	-0.13	-0.14	-0.06	$\tau_1 = 0.9$	-0.02	0.05	0.12
Male				Male			
$\mathcal{C}_1$	$\tau_2$	$\tau_2$	$\tau_2$	$\mathcal{C}_2$	$\tau_2$	$\tau_2$	$\tau_2$
	0.1	0.5	0.9		0.1	0.5	0.9
$\tau_1 = 0.1$	-0.03	-0.09	-0.12	$\tau_1 = 0.1$	0.30	-0.02	-0.40
$\tau_1 = 0.5$	-0.07	-0.08	-0.08	$\tau_1 = 0.5$	-0.05	-0.19	-0.10
$\tau_1 = 0.9$	-0.11	-0.05	-0.03	$\tau_1 = 0.9$	-0.42	-0.16	0.32

the male population involves the same number of groups than the one for the total population, both partitions are substantially different. In fact, the solution for the male population includes a cluster  $\mathcal{C}_1$  containing all the countries except for ISL, which is the medoid of cluster  $\mathcal{C}_2$ , thus indicating that the male mortality data of this country are dramatically different from the rest in terms of serial dependence patterns. On the other hand, the solution for the female population is quite difficult to interpret, since it involves six groups.

The weighted averages of the corresponding FQA-based features for the male and female data are provided in the bottom part of Table 9 and in Table 1 of the Supplementary Material, respectively. Note that, for the male population, some quantities associated with cluster  $\mathcal{C}_2$  are quite large in absolute value, implying that the male mortality data of ISL exhibit a substantially stronger degree of serial dependence than the ones displayed by its counterparts. On the other hand, for the female population, the six clusters are associated with different dependence patterns, and, in all cases, the groups display a stronger degree of dependence at the first lag ( $l = 1$ ) than at the second lag ( $l = 2$ ).

## 6 Conclusions


We introduced a distance between functional time series based on a new measure of serial dependence which can be seen as an extension of the classical quantile autocorrelation function to the functional setting. We called this measure the functional quantile autocorrelation. A clustering procedure for functional time series was constructed by using the proposed distance in combination with the classical fuzzy  $C$ -medoids algorithm, which allows for the assignment of gradual memberships of the series to the different groups. This is particularly useful when dealing with time series datasets, where different amounts of dissimilarity between the underlying processes or changes in the dynamic behaviors over time are frequent. The algorithm involves some hyperparameters whose selection can be properly carried out using criteria based on hypothesis testing and internal clustering quality indexes.

To evaluate the performance of the proposed procedure, several simulations were carried out involving scenarios formed by functional time series belonging to well-separated clusters and scenarios including a certain amount of uncertainty. Different classes of functional processes were considered. The algorithm was compared with several alternative clustering procedures. Specifically, we considered the fuzzy  $C$ -medoids algorithm based on two metrics relying on functional autocorrelations and one procedure that employs functional panel data modeling. The proposed clustering technique: (i) shows competitive results with databases containing linear time series, being even able to outperform autocorrelation-based methods when the dataset includes ambiguous time series, and (ii) displays a substantially higher clustering accuracy than the alternative approaches when the underlying clusters are characterized by complex forms of functional dependence. Also, the approach is computationally efficient.

The usefulness of the clustering algorithm was illustrated using of two applications involving time series of stock returns and mortality improvement rates. Specifically, the first case study considered functional time series of daily curves of 5-minute returns for several American companies belonging to two different sectors. We showed that the procedure can differentiate between both sectors to some extent, with some time series displaying a considerable fuzzy behavior. The second case study involved functional time series of yearly curves of mortality improvement rates for different countries. The resulting clustering partition lead to an interesting interpretation related to certain characteristics of the considered countries. These applications indicated that: (i) the proposed measure of serial dependence can provide a significant understanding of the nature of the time series under study, and (ii) the clustering algorithm can produce a meaningful partition whose membership degrees give insights to practitioners about certain time series in the dataset.

There are several ways in which this work can be further extended, and we list five below: 1) Robust versions of the proposed technique can be constructed by considering the so-called metric, noise, and trimmed approaches (Lafuente-Rego et al. 2020, D’Urso et al. 2016, López-Oriona, D’Urso, Vilar and Lafuente-Rego 2022a), which adapt the objective function of the algorithm in a proper manner so that outliers do not negatively affect the resulting partition. 2) A spatial penalization term could be incorporated in the objective function of the procedure to deal with functional time series datasets containing geographical information (Coppi et al. 2010, López-Oriona, D’Urso, Vilar and Lafuente-Rego 2022b). 3) A spectral counterpart of the functional quantile autocorrelation giving frequency information about the functional time series could be defined. Such a measure could lead to the construction of frequency domain clustering algorithms (Maharaj and D’Urso 2011, López-Oriona and Vilar 2021). 4) The asymptotic properties of the functional quantile autocorrelation could be derived under certain hypotheses. 5) Statistical tests for the null hypothesis of i.i.d. functional data could be constructed by considering statistics based on the functional quantile autocorrelation. It would be interesting to address these topics in future research.

## SUPPLEMENTARY MATERIAL

**R code for clustering high-dimensional functional time series** The  code used for Monte-Carlo simulation studies and empirical application is available in [https://github.com/anloor7/PostDoc/tree/main/r\\_code/functional](https://github.com/anloor7/PostDoc/tree/main/r_code/functional).

**Supplement file** The supplement file contains a table with the weighted averages of the FQA-based features associated with the six-cluster solution for the female FTS in the application of Section 5.2.

## Supplement to “Dependence-based fuzzy clustering of functional time series”

Table 10 contains the weighted averages of the FQA-based features associated with the six-cluster solution for the female functional time series in the application of Section 5.2.

Table 10: Values of  $\bar{\rho}_c(\tau_1, \tau_2, 1, \tau_1, \tau_2)$  and  $\bar{\rho}_c(\tau_1, \tau_2, 2, \tau_1, \tau_2)$  for the six-cluster solution produced by  $\hat{d}_{\text{FQA}}$  with the 33 functional time series of mortality improvement rates for the female population.

$l = 1$				$l = 2$			
$\mathcal{C}_1$	0.1	$\tau_2$ 0.5	0.9	$\mathcal{C}_1$	0.1	$\tau_2$ 0.5	0.9
$\tau_1 = 0.1$	-0.06	-0.20	-0.21	$\tau_1 = 0.1$	-0.01	0.00	-0.03
$\tau_1 = 0.5$	-0.18	-0.25	-0.16	$\tau_1 = 0.5$	-0.04	-0.04	-0.05
$\tau_1 = 0.9$	-0.20	-0.20	-0.09	$\tau_1 = 0.9$	-0.04	-0.02	-0.05
$\mathcal{C}_2$	0.1	$\tau_2$ 0.5	0.9	$\mathcal{C}_2$	0.1	$\tau_2$ 0.5	0.9
$\tau_1 = 0.1$	-0.04	-0.10	-0.03	$\tau_1 = 0.1$	0.02	0.02	-0.02
$\tau_1 = 0.5$	-0.08	-0.09	0.00	$\tau_1 = 0.5$	0.06	0.07	0.00
$\tau_1 = 0.9$	-0.17	-0.07	0.00	$\tau_1 = 0.9$	0.03	0.06	-0.04
$\mathcal{C}_3$	0.1	$\tau_2$ 0.5	0.9	$\mathcal{C}_3$	0.1	$\tau_2$ 0.5	0.9
$\tau_1 = 0.1$	-0.02	-0.13	-0.11	$\tau_1 = 0.1$	0.02	0.00	0.01
$\tau_1 = 0.5$	-0.17	-0.25	-0.12	$\tau_1 = 0.5$	-0.03	0.01	-0.03
$\tau_1 = 0.9$	-0.30	-0.26	-0.09	$\tau_1 = 0.9$	-0.02	0.05	-0.03
$\mathcal{C}_4$	0.1	$\tau_2$ 0.5	0.9	$\mathcal{C}_4$	0.1	$\tau_2$ 0.5	0.9
$\tau_1 = 0.1$	0.00	-0.18	-0.14	$\tau_1 = 0.1$	0.15	0.03	-0.08
$\tau_1 = 0.5$	-0.12	-0.25	-0.10	$\tau_1 = 0.5$	0.10	0.04	-0.14
$\tau_1 = 0.9$	-0.22	-0.19	-0.05	$\tau_1 = 0.9$	0.13	0.12	-0.05
$\mathcal{C}_5$	0.1	$\tau_2$ 0.5	0.9	$\mathcal{C}_5$	0.1	$\tau_2$ 0.5	0.9
$\tau_1 = 0.1$	-0.08	-0.18	-0.23	$\tau_1 = 0.1$	0.15	0.11	0.02
$\tau_1 = 0.5$	-0.16	-0.24	-0.18	$\tau_1 = 0.5$	0.06	0.02	-0.04
$\tau_1 = 0.9$	-0.20	-0.18	-0.03	$\tau_1 = 0.9$	-0.02	0.00	0.02
$\mathcal{C}_6$	0.1	$\tau_2$ 0.5	0.9	$\mathcal{C}_6$	0.1	$\tau_2$ 0.5	0.9
$\tau_1 = 0.1$	-0.11	-0.18	-0.23	$\tau_1 = 0.1$	0.18	0.09	0.04
$\tau_1 = 0.5$	-0.27	-0.28	-0.22	$\tau_1 = 0.5$	0.08	0.06	0.11
$\tau_1 = 0.9$	-0.30	-0.21	-0.09	$\tau_1 = 0.9$	0.00	0.06	0.17

## Acknowledgment

The first two authors thank the support from the King Abdullah University of Science and Technology (KAUST). The last author thanks the financial support from an Australian Research Council Discovery Project DP230102250.

## References

- Aghabozorgi, S., Shirkhorshidi, A. S. and Wah, T. Y. (2015), 'Time-series clustering—a decade review', *Information systems* **53**, 16–38.
- Arabie, P., Carroll, J. D., DeSarbo, W. and Wind, J. (1981), 'Overlapping clustering: A new method for product positioning', *Journal of Marketing Research* **18**(3), 310–317.
- Aue, A., Horváth, L. and F. Pellatt, D. (2017), 'Functional generalized autoregressive conditional heteroskedasticity', *Journal of Time Series Analysis* **38**(1), 3–21.
- Bezdek, J. C. (2013), *Pattern Recognition with Fuzzy Objective Function Algorithms*, Springer, New York.
- Booth, G. G., Martikainen, T., Sarkar, S. K., Virtanen, I. and Yli-Olli, P. (1994), 'Nonlinear dependence in Finnish stock returns', *European Journal of Operational Research* **74**(2), 273–283.
- Bosq, D. (2000), *Linear Processes in Function Spaces: Theory and Applications*, Vol. 149, Springer, New York.
- Bouveyron, C., Côme, E. and Jacques, J. (2015), 'The discriminative functional mixture model for a comparative analysis of bike sharing systems', *The Annals of Applied Statistics* **9**(4), 1726–1760.
- Bouveyron, C. and Jacques, J. (2011), 'Model-based clustering of time series in group-specific functional subspaces', *Advances in Data Analysis and Classification* **5**(4), 281–300.
- Campello, R. J. (2007), 'A fuzzy extension of the rand index and other related indexes for clustering and classification assessment', *Pattern Recognition Letters* **28**(7), 833–841.
- Cerqueti, R., D'Urso, P., De Giovanni, L., Mattera, R. and Vitale, V. (2022), 'INGARCH-based fuzzy clustering of count time series with a football application', *Machine Learning with Applications* **10**, 100417.

- Chamroukhi, F. and Nguyen, H. D. (2019), 'Model-based clustering and classification of functional data', *Wiley Interdisciplinary Reviews: Data Mining and Knowledge Discovery* **9**(4), e1298.
- Chamroukhi, F., Pham, N. T., Hoang, V. H. and McLachlan, G. J. (2024), 'Functional mixtures-of-experts', *Statistics and Computing* **34**(Article number 98).
- Chen, C. W., So, M. K. and Gerlach, R. H. (2005), 'Assessing and testing for threshold nonlinearity in stock returns', *Australian & New Zealand Journal of Statistics* **47**(4), 473–488.
- Chiou, J.-M. and Li, P.-L. (2007), 'Functional clustering and identifying substructures of longitudinal data', *Journal of the Royal Statistical Society: Series B* **69**(4), 679–699.
- Coppi, R., D'Urso, P. and Giordani, P. (2010), 'A fuzzy clustering model for multivariate spatial time series', *Journal of Classification* **27**(1), 54–88.
- Corduas, M. and Piccolo, D. (2008), 'Time series clustering and classification by the autoregressive metric', *Computational Statistics & Data Analysis* **52**(4), 1860–1872.
- Dahmene, M., Boughrara, A. and Slim, S. (2021), 'Nonlinearity in stock returns: Do risk aversion, investor sentiment and, monetary policy shocks matter?', *International Review of Economics & Finance* **71**, 676–699.
- Dunn, J. C. (1973), 'A fuzzy relative of the isodata process and its use in detecting compact well-separated clusters', *Journal of Cybernetics* **3**, 32–57.
- D'Urso, P., De Giovanni, L. and Massari, R. (2016), 'GARCH-based robust clustering of time series', *Fuzzy Sets and Systems* **305**, 1–28.
- D'Urso, P. and Maharaj, E. A. (2012), 'Wavelets-based clustering of multivariate time series', *Fuzzy Sets and Systems* **193**, 33–61.
- D'Urso, P., Di Lallo, D. and Maharaj, E. A. (2013), 'Autoregressive model-based fuzzy clustering and its application for detecting information redundancy in air pollution monitoring networks', *Soft Computing* **17**(1), 83–131.
- D'Urso, P. and Maharaj, E. A. (2009), 'Autocorrelation-based fuzzy clustering of time series', *Fuzzy Sets and Systems* **160**(24), 3565–3589.
- Etienne, C. and Latifa, O. (2014), 'Model-based count series clustering for bike sharing system usage mining: A case study with the Velib system of Paris', *ACM Transactions on Intelligent Systems and Technology (TIST)* **5**(3), 1–21.

- Febrero-Bande, M. and Oviedo de la Fuente, M. (2012), 'Statistical computing in functional data analysis: The R package *fda.usc*', *Journal of Statistical Software* **51**(4), 1–28.
- Frühwirth-Schnatter, S. and Pamminger, C. (2010), 'Model-based clustering of categorical time series', *Bayesian Analysis* **5**(2), 345–368.
- Gao, Y., Shang, H. L. and Yang, Y. (2019), 'High-dimensional functional time series forecasting: An application to age-specific mortality rates', *Journal of Multivariate Analysis* **170**, 232–243.
- Garcia-Escudero, L. A. and Gordaliza, A. (2005), 'A proposal for robust curve clustering', *Journal of Classification* **22**(2), 185–201.
- García-Magariños, M. and Vilar, J. A. (2015), 'A framework for dissimilarity-based partitioning clustering of categorical time series', *Data mining and knowledge discovery* **29**(2), 466–502.
- Guo, S., Qiao, X. and Wang, Q. (2022), Factor modelling for high-dimensional functional time series, Technical report, arXiv.  
**URL:** <https://arxiv.org/abs/2112.13651>
- Haberman, S. and Renshaw, A. (2012), 'Parametric mortality improvement rate modelling and projecting', *Insurance: Mathematics and Economics* **50**(3), 309–333.
- Hinich, M. J. and Patterson, D. M. (1985), 'Evidence of nonlinearity in daily stock returns', *Journal of Business & Economic Statistics* **3**(1), 69–77.
- Höppner, F., Klawonn, F., Kruse, R. and Runkler, T. (1999), *Fuzzy Cluster Analysis: Methods for Classification, Data Analysis and Image Recognition*, John Wiley & Sons, Chichester.
- Hörmann, S. and Kokoszka, P. (2010), 'Weakly dependent functional data', *The Annals of Statistics* **38**, 1845–1884.
- Hörmann, S. and Kokoszka, P. (2012), Functional time series, in T. S. Rao, S. S. Rao and C. R. Rao, eds, 'Handbook of Statistics', Vol. 30, Elsevier, pp. 157–186.
- Horváth, L., Kokoszka, P. and Rice, G. (2014), 'Testing stationarity of functional time series', *Journal of Econometrics* **179**(1), 66–82.
- Huang, X. and Shang, H. L. (2023), 'Nonlinear autocorrelation function of functional time series', *Nonlinear Dynamics* **111**(3), 2537–2554.

Human Mortality Database (2024), *University of California, Berkeley (USA), and Max Planck Institute for Demographic Research (Germany)*. Data downloaded on 31 January 2024.

URL: [www.mortality.org](http://www.mortality.org)

Hyndman, R. (2023), *demography: Forecasting Mortality, Fertility, Migration and Population Data*. R package version 2.0.

URL: <https://CRAN.R-project.org/package=demography>

Hyndman, R. J. and Shang, H. L. (2009), 'Forecasting functional time series', *Journal of the Korean Statistical Society* **38**(3), 199–211.

Hyndman, R. and Shang, H. L. (2024), *ftsa: Functional Time Series Analysis*. R package version 6.4.

URL: <https://CRAN.R-project.org/package=ftsa>

Izakian, H., Pedrycz, W. and Jamal, I. (2015), 'Fuzzy clustering of time series data using dynamic time warping distance', *Engineering Applications of Artificial Intelligence* **39**, 235–244.

Jacques, J. and Preda, C. (2014), 'Model-based clustering for multivariate functional data', *Computational Statistics & Data Analysis* **71**, 92–106.

Kaufman, L. and Rousseeuw, P. J. (2009), *Finding Groups in Data: An Introduction to Cluster Analysis*, John Wiley & Sons, New York.

Kim, M. and Kokoszka, P. (2022), 'Extremal dependence measure for functional data', *Journal of Multivariate Analysis* **189**, 104887.

Kokoszka, P. and Zhang, X. (2012), 'Functional prediction of intraday cumulative returns', *Statistical Modelling* **12**(4), 377–398.

Krishnapuram, R., Joshi, A. and Yi, L. (1999), A fuzzy relative of the k-medoids algorithm with application to web document and snippet clustering, in 'FUZZ-IEEE'99. 1999 IEEE International Fuzzy Systems. Conference Proceedings (Cat. No. 99CH36315)', Vol. 3, IEEE, pp. 1281–1286.

Lafuente-Rego, B., D'Urso, P. and Vilar, J. A. (2020), 'Robust fuzzy clustering based on quantile autocovariances', *Statistical Papers* **61**(6), 2393–2448.

Lafuente-Rego, B. and Vilar, J. A. (2016), 'Clustering of time series using quantile autocovariances', *Advances in Data Analysis and Classification* **10**(3), 391–415.



- Lee, J. and Rao, S. S. (2011), The quantile spectral density and comparison based tests for nonlinear time series, Technical report, arXiv.  
URL: <https://arxiv.org/abs/1112.2759>
- Liao, T. W. (2005), 'Clustering of time series data—a survey', *Pattern Recognition* **38**(11), 1857–1874.
- Linton, O. and Whang, Y.-J. (2007), 'The quantilogram: With an application to evaluating directional predictability', *Journal of Econometrics* **141**(1), 250–282.
- López-Oriona, Á., D'Urso, P., Vilar, J. A. and Lafuente-Rego, B. (2022a), 'Quantile-based fuzzy C-means clustering of multivariate time series: Robust techniques', *International Journal of Approximate Reasoning* **150**, 55–82.
- López-Oriona, Á., D'Urso, P., Vilar, J. A. and Lafuente-Rego, B. (2022b), 'Spatial weighted robust clustering of multivariate time series based on quantile dependence with an application to mobility during covid-19 pandemic', *IEEE Transactions on Fuzzy Systems* **30**(9), 3990–4004.
- López-Oriona, Á. and Vilar, J. A. (2021), 'Quantile cross-spectral density: A novel and effective tool for clustering multivariate time series', *Expert Systems with Applications* **185**, 115677.
- López-Oriona, Á., Vilar, J. A. and D'Urso, P. (2022), 'Quantile-based fuzzy clustering of multivariate time series in the frequency domain', *Fuzzy Sets and Systems* **443**, 115–154.
- López-Oriona, Á., Vilar, J. A. and D'Urso, P. (2023), 'Hard and soft clustering of categorical time series based on two novel distances with an application to biological sequences', *Information Sciences* **624**, 467–492.
- López-Oriona, Á., Weiß, C. H. and Vilar, J. A. (2023), 'Two novel distances for ordinal time series and their application to fuzzy clustering', *Fuzzy Sets and Systems* **468**, 108590.
- Łuczak, M. (2016), 'Hierarchical clustering of time series data with parametric derivative dynamic time warping', *Expert Systems with Applications* **62**, 116–130.
- Maharaj, E. A., D'Urso, P. and Caiado, J. (2019), *Time Series Clustering and Classification*, Chapman and Hall/CRC, Boca Raton, Florida.
- Maharaj, E. A. and D'Urso, P. (2011), 'Fuzzy clustering of time series in the frequency domain', *Information Sciences* **181**(7), 1187–1211.

- Martínez-Hernández, I. and Genton, M. G. (2021), 'Nonparametric trend estimation in functional time series with application to annual mortality rates', *Biometrics* **77**(3), 866–878.
- Miyamoto, S., Ichihashi, H., Honda, K. and Ichihashi, H. (2008), *Algorithms for Fuzzy Clustering: Methods in c-Means Clustering with Applications*, Vol. 10, Springer, Berlin, Heidelberg.
- Pealat, C., Bouleux, G. and Cheutet, V. (2021), Improved time-series clustering with UMAP dimension reduction method, in '2020 25th International Conference on Pattern Recognition (ICPR)', IEEE, Milan, Italy, pp. 5658–5665.
- R Core Team (2024), *R: A Language and Environment for Statistical Computing*, R Foundation for Statistical Computing, Vienna, Austria.  
URL: <https://www.R-project.org/>
- Ramsay, J. O. and Silverman, B. W. (2005), *Functional Data Analysis*, Springer, New York.
- Shang, H. L. (2019), 'Dynamic principal component regression: Application to age-specific mortality forecasting', *ASTIN Bulletin* **49**(3), 619–645.
- Singhal, A. and Seborg, D. E. (2005), 'Clustering multivariate time-series data', *Journal of Chemometrics* **19**(8), 427–438.
- Székely, G. J. and Rizzo, M. L. (2013), 'The distance correlation t-test of independence in high dimension', *Journal of Multivariate Analysis* **117**, 193–213.
- Tang, C., Shang, H. L. and Yang, Y. (2022), 'Clustering and forecasting multiple functional time series', *The Annals of Applied Statistics* **16**(4), 2523–2553.
- Tarpey, T. and Kinatader, K. K. (2003), 'Clustering functional data', *Journal of Classification* **20**(1), 93–114.
- Valencia, D., Lillo, R. E. and Romo, J. (2019), 'A Kendall correlation coefficient between functional data', *Advances in Data Analysis and Classification* **13**, 1083–1103.
- Vilar, J. A., Lafuente-Rego, B. and D'Urso, P. (2018), 'Quantile autocovariances: A powerful tool for hard and soft partitional clustering of time series', *Fuzzy Sets and Systems* **340**, 38–72.
- Wang, H. and Cao, J. (2023), 'Nonlinear prediction of functional time series', *Environmetrics* **34**(5), e2792.

Wang, J.-L., Chiou, J.-M. and Müller, H.-G. (2016), 'Functional data analysis', *Annual Review of Statistics and Its Application* **3**, 257–295.

Xie, X. L. and Beni, G. (1991), 'A validity measure for fuzzy clustering', *IEEE Transactions on Pattern Analysis & Machine Intelligence* **13**(08), 841–847.